

UC Riverside

UC Riverside Electronic Theses and Dissertations

Title

Noncuring Graphene Thermal Interface Materials for Advanced Electronics

Permalink

<https://escholarship.org/uc/item/708332gw>

Author

Naghibi, Sahar

Publication Date

2020

Copyright Information

This work is made available under the terms of a Creative Commons Attribution-NonCommercial-NoDerivatives License, available at <https://creativecommons.org/licenses/by-nc-nd/4.0/>

Peer reviewed|Thesis/dissertation

UNIVERSITY OF CALIFORNIA
RIVERSIDE

Noncuring Graphene Thermal Interface Materials for Advanced Electronics

A Dissertation submitted in partial satisfaction
of the requirements for the degree of

Doctor of Philosophy

in

Materials Science and Engineering

by

Sahar Naghibi

March 2020

Dissertation Committee:

Dr. Alexander Balandin, Chairperson

Dr. Alexander Khitun

Dr. Fariborz Kargar

Copyright by
Sahar Naghibi
2020

The Dissertation of Sahar Naghibi is approved:

Committee Chairperson

University of California, Riverside

Acknowledgements

Thank you to all who I met during my graduate program, all of whom helped shape who I am as a person, engineer and scientist.

First, I would like to thank my advisor Dr. Alexander Balandin, his encouragement, guidance and positive motivation made even the most difficult scientific problems although challenging, seem easy and fun. I had the opportunity to attend conferences, present my work as well develop my own methods for conducting experiments. The environment he has created and nurtures in his group is one where curiosity and creativity flourish, and its product is bleeding edge research. I am very thankful to have him as a mentor.

I would also like to thank Dr. Fariborz Kargar (Fari) for his patience, kindness and guidance during my time in the Nano Device Lab (NDL) and Phonon Optimized Engineered Materials (POEMs) lab. Thank you to Dr. Alexander Khitun for agreeing to serve on my dissertation committee. Someone once said if you do what you love you'll never work a day in your life, what they forgot is that it's who you work *with* that matters the most. My NDL/POEMs lab mates past and present as well as my past labmates I would like to thank you all for making working with you all so easy that I didn't know I was at work. Thank you all: Tammy Huang, Ruben Salgado, Dylan Wright, Zahra Barani, Amirmahdi Mohammadzadeh, Ece Aytan, Jacob Lewis, Fariborz Kargar, Subhajit Ghosh, Barath Mahadevan, Ariana Nyguen, Thomas Empante, Michael Valentin, David Barroso. I would also like to thank Velveth Klee, my first mentor and lifelong friend. To the coffee Thursdays with Velveth and always being around in a moments notice, thank you. Another

friend I would also like to thank Zaira Alibay your positive outlook on life and can do attitude was motivation to go to the gym and work through problems both in the classroom and lab. To Robert, thanks. I would also like to thank the friends I made a long and who have helped me: Angela Villanueva, Brandon Davis, Melissa Ramos. I would also like to thank my former advisor Dr. Ludwig Bartels for the opportunity to work in his lab and always challenging me.

Lastly and most importantly, I would like to thank my family my mother, Silvia L. Naghibi, father, Bahram Naghibi, and sister, Ariana Naghibi without their sacrifices, love, and support none of this would be possible. Thank you.

Parts of this dissertation were written based on or reprinted from previously published materials as it is presented in the following journals:

Naghibi, S., Kargar, F., Wright, D., Huang, C. Y. T., Mohammadzadeh, A., Barani, Z., Salgado, R. & Balandin, A. A. Noncuring Graphene Thermal Interface Materials for Advanced Electronics. *Advanced Electronic Materials* 1901303 (2020). doi:10.1002/aelm.201901303

Naghibi, S.; Kargar, F.; Barani, Z.; Salgado, R.; Wright, D.; Balandin, A. A. “Non-Cured Thermal Interface Materials with High Graphene Loading”, Oral Presentation given at Materials Research Society Conference Spring 2019; Phoenix, Arizona; 25 April 2019.

*Dedicated
to my
Mother and Father*

ABSTRACT OF DISSERTATION

Noncuring Graphene Thermal Interface Materials for Advanced Electronics

by

Sahar Naghibi

Doctor of Philosophy, Graduate Program in Materials Science and Engineering

University of California, Riverside, March 2020

Dr. Alexander A. Balandin

As transistors continue to decrease in size and packing densities increase, thermal management becomes a critical bottleneck for development of the next generation of compact and flexible electronics. The increase in computer usage and ever-growing dependence on cloud systems require better methods for dissipating heat away from electronic components. The important ingredients of thermal management are the thermal interface materials. The discovery of excellent heat conduction properties of graphene and few-layer graphene stimulated research on practical applications of graphene fillers in thermal interface materials. The initial studies of graphene fillers in thermal interface materials were focused almost exclusively on curing epoxy-based composites. However, many thermal management applications require specifically noncuring thermal paste type materials. This dissertation reports on the synthesis and thermal conductivity measurements of noncuring thermal paste based on mineral oil with the mixture of graphene and few-layer graphene flakes as the fillers. The relatively simple composition has been selected in order to systematically compare the performance and understand the mechanisms governing heat conduction. It was found that graphene thermal paste exhibits

a distinctive thermal percolation threshold with the thermal conductivity revealing a sublinear dependence on the filler loading. This behavior contrasts with the thermal conductivity of curing graphene thermal interface materials, based on epoxy, where super-linear dependence on the filler loading is observed. The performance of graphene thermal paste was benchmarked against top-of-the-line commercial thermal pastes. The obtained results show that noncuring graphene thermal interface materials outperforms the best commercial pastes in terms of thermal conductivity, at substantially lower filler concentration. The results of this dissertation research shed light on the thermal percolation mechanism in noncuring polymeric matrices laden with quasi-two-dimensional fillers. Considering recent progress in graphene production *via* liquid phase exfoliation and oxide reduction, it is possible that the undertaken approach will open a pathway for large-scale industrial application of graphene in thermal management of electronics.

Table of Contents

Chapter 1: Introduction.....	1
1.2 Historical Perspective.....	2
References	5
Chapter 2: Phonons, Thermal Conductivity and Thermal Management.....	9
2.1 Introduction	9
2.2 Graphene	10
2.3 Thermal Management	11
2.4 Phonons and Thermal Conductivity.....	13
2.5 Thermal Interface Materials	14
2.6 Summary	17
References	18
Chapter 3: Sample Preparation and Thermal Conductivity Measurement	
Tools	21
3.1 Introduction	21
3.2 Steady State Thermal Conductivity Measurement Method	21
3.2.1 Theory of the Steady State Method	22
3.3 Sample Preparation	26
3.4 Scanning Electron Microscopy Characterization.....	29
3.5 Raman Spectroscopy	31
3.6 Rheological Properties of Non-Graphene TIMs	32
3.7 Summary and Conclusions.....	37
References	39

Chapter 4: Noncuring Graphene Thermal Interface Materials for Advanced Electronics	41
4.1 Introduction	41
4.2 Material Synthesis and Characterization.....	46
4.3 Results of Thermal Testing	49
4.4 Benchmarking Against Commercial Noncuring TIMs	59
4.5 Conclusion.....	62
References	63

List of Figures

Figure 2.1: The various industries which are dependent on advancements in TIMs. (Clockwise from top) Medical devices and wearables, computers and handhelds, telecommunication, solar panel advancement and electric vehicles.....	12
Figure 2.2: Thermal interface materials are at the center of thermal management of most electronics, they bind two uneven surfaces, such as a die and heat sink (shown above). They reduce thermal resistance between the two uneven surfaces which they bind.	15
Figure 2.3: Subgroups of thermal interface materials which include <i>noncuring</i> , <i>phase change materials</i> , and <i>curing</i> (clockwise). Applications for TIMs continues to grow and includes automobiles, consumer electronics and wearables.	16
Figure 3.1: TIM tester (LonGwin) used to conduct all thermal measurements for noncuring thermal interface materials used. This instrument allows for various aspects to be controlled while measuring including pressure, temperature control of measurements. Nanofabrication Facility, UC Riverside, 2019.	24
Figure 3.2: Schematic of TIM tester (LonGwin). A sample is placed in between two plates labeled T_d and T_c and measured at varying thicknesses. Standard steady state ASTM testing setup.	25
Figure 3.3: Process flow of sample preparation for noncuring graphene TIMs.	27
Table 3.1: Effect of various preparation parameters on the thermal conductivity of the TIMs with 20 wt% of graphene filler loading kept constant.	29
Figure 3.4: SEM images show graphene flakes in noncuring TIM paste.	30
Figure 3.5: Raman spectra of noncuring graphene thermal interface material, with a weight fraction of 40 wt% graphene fillers. Raman was used to verify the homogeneity of the graphene within the TIM post material development.	32
Figure 3.6: Relationship between shear stress and shear rate for various Newtonian and non-Newtonian fluids. The relationship between these two observations is used to define the robustness and longevity of a TIM.	34
Figure 3.7: Rheological properties of the mineral oil confirming its Newtonian fluid behavior.....	35

Figure 3.8: Rheological properties of mineral oil with 5 wt% of graphene. The results show a sup-linear behavior of shear stress as a function of shear rate confirming the pseudo plastic properties of the compound. 36

Figure 3.9: Rheological properties of the mineral oil with 10 wt% of graphene loading. The results show a linear behavior of shear stress as a function of shear rate with a positive y-intercept confirming the Bingham plastic behavior of the compound, where an initial stress must be applied for the substance to become liquid. 37

Figure 4.2: The above schematic highlights the resistance which two uneven surfaces creates with respect to the TIM and the direction of the heat flux. Reprinted with permission from Advanced Electronic Materials. The data is from Naghibi, S., Kargar, F., Wright, D., Huang, C. Y. T., Mohammadzadeh, A., Barani, Z., Salgado, R. & Balandin, A. A. Noncuring Graphene Thermal Interface Materials for Advanced Electronics. *Advanced Electronic Materials* 1901303 (2020). doi:10.1002/aelm.201901303..... 50

Figure 4.3: Thermal resistance per unit area, R'' , as a function of the bond line thickness. The dashed lines show the linear regression fittings to the experimental data. Adding graphene fillers to mineral oil results in the slope of the lines decreasing significantly, indicating string enhancement in the “bulk” thermal conductivity of the graphene thermal paste. Reprinted with permission from Advanced Electronic Materials. The data is from Naghibi, S., Kargar, F., Wright, D., Huang, C. Y. T., Mohammadzadeh, A., Barani, Z., Salgado, R. & Balandin, A. A. Noncuring Graphene Thermal Interface Materials for Advanced Electronics. *Advanced Electronic Materials* 1901303 (2020). doi:10.1002/aelm.201901303. 51

Figure 4.4: Thermal conductivity of the noncuring graphene TIMs as a function of graphene volume fraction. Adding fillers to the mineral oil base leads to more than 4× enhancement of the thermal conductivity at $\phi = 1.9$ vol%. The strong enhancement is attributed to the onset of the thermal percolation. The increase in thermal conductivity slows down as more fillers are incorporated into the matrix, and it saturates at the high loading fractions. The dashed lines are the theoretical fitting of the experimental data according to the effective thermal conductivity equation $k \sim \phi - \phi_{th}^p$ with $\phi_{th} = 1.9$ vol% and $p = 0.32$. The inset shows the data in a log-log scale. Reprinted with permission from Advanced Electronic Materials. The data is from Naghibi, S., Kargar, F., Wright, D., Huang, C. Y. T., Mohammadzadeh, A., Barani, Z., Salgado, R. & Balandin, A. A. Noncuring Graphene Thermal Interface Materials for Advanced Electronics. *Advanced Electronic Materials* 1901303 (2020). doi:10.1002/aelm.201901303..... 53

Figure 4.5: Thermal contact resistance as a function of the filler loading. The error bars show the standard error. The thermal contact resistance increases with the loading fraction. Reprinted with permission from Advanced Electronic Materials. The data is from Naghibi,

S., Kargar, F., Wright, D., Huang, C. Y. T., Mohammadzadeh, A., Barani, Z., Salgado, R. & Balandin, A. A. Noncuring Graphene Thermal Interface Materials for Advanced Electronics. *Advanced Electronic Materials* 1901303 (2020). doi:10.1002/aelm.201901303. 55

Figure 4.6: “Apparent” thermal conductivity of the non-cured graphene TIMs as a function of temperature in the range from 40 °C to 115 °C. Reprinted with permission from Advanced Electronic Materials. The data is from Naghibi, S., Kargar, F., Wright, D., Huang, C. Y. T., Mohammadzadeh, A., Barani, Z., Salgado, R. & Balandin, A. A. Noncuring Graphene Thermal Interface Materials for Advanced Electronics. *Advanced Electronic Materials* 1901303 (2020). doi:10.1002/aelm.201901303..... 57

Figure 4.7: Bond line thickness as a function of temperature at atmospheric pressure. The variation in BLT for mineral oil and noncuring graphene TIM with $\phi = 1.9$ vol% is ~ 2.3 $\mu\text{m}/^\circ\text{C}$. The variation in the TIM thickness with temperature drops to ~ 0.5 $\mu\text{m}/^\circ\text{C}$ at the higher graphene filler loading. The latter indicates the noncuring graphene TIMs with higher graphene loading are less prone to the “bleeding-out” problem. Reprinted with permission from Advanced Electronic Materials. The data is from Naghibi, S., Kargar, F., Wright, D., Huang, C. Y. T., Mohammadzadeh, A., Barani, Z., Salgado, R. & Balandin, A. A. Noncuring Graphene Thermal Interface Materials for Advanced Electronics. *Advanced Electronic Materials* 1901303 (2020). doi:10.1002/aelm.201901303..... 58

Figure 4.8: Benchmarking of noncuring graphene TIMs against commercial noncuring TIMs. The noncuring graphene TIM has $\phi = 19.8$ vol% (40 wt%) filler loading. The grey bars show the thermal conductivity values claimed by the vendors. The light coral bars present the data measured by the same instrument used for this study. There is a substantial discrepancy between the claimed and measured data for the commercial TIMs. The noncuring graphene thermal paste outperforms all commercial noncuring TIMs. A commercial noncuring TIM with the highest thermal conductivity (PK Pro-3) uses ~ 90 wt% of Al and ZnO filler loading, which is more than two times of the graphene filler concentration used in this study. Reprinted with permission from Advanced Electronic Materials. The data is from Naghibi, S., Kargar, F., Wright, D., Huang, C. Y. T., Mohammadzadeh, A., Barani, Z., Salgado, R. & Balandin, A. A. Noncuring Graphene Thermal Interface Materials for Advanced Electronics. *Advanced Electronic Materials* 1901303 (2020). doi:10.1002/aelm.201901303..... 60

Table 4.1: Thermal conductivity of noncuring thermal interface materials with different fillers. 61

Chapter 1: Introduction

The increase in chip density and processing power has allowed for peak optimization which have led towards IoT, 5G and autonomous vehicles (AV). The Internet of Things (IoT) promises to connect all electronic and non-electronic components (including people and animals) to a wireless network where data can be transferred between systems, seamlessly.¹⁻³ The many benefits do not offset all of the limits in regards to the processing power needed, and the rigorous thermal conditions which these devices experience. The increase in chip density and complexity have created various road blocks in both processing and functionality. One of these very real problems is removal of excess heat created within these intricate stackings.⁴⁻⁶ Thermal Interface Materials (TIM) interface two uneven solid surfaces where air would be a poor conductor of heat, they aid in the transfer of heat from one medium into another. Although the approach of on-chip design for better thermal dissipation is an option, it is still limited by material function and the ever-increasing transistor density per chip.^{4,7,8} Previously noted that even with a change in design, thermal limits are quickly caught up to and largely exceeded.⁹⁻¹¹ High performance chipsets together with a high-speed network make 5G and IoT thermal obstacles. It is estimated that by 2025 devices related to IoT functions, from data center usage to an idle handheld, will consume about 25% of the power produced worldwide.¹² Currently, 4% of the total energy consumed by the United States is used to power large data centers, of that amount about half is used to cool them. One can easily imagine the amount which would be needed to cool the various electronics used IoT from phones, tablets and computer to automobile

systems. The demands which these new technologies have made in chip design as well connectivity to a larger network is the fuel for this work.

The emergence of graphene set in motion a surge of research with promise in various fields and markets. Its high electrical conductivity and two-dimensional nature^{13–16} made it a promising for use as interconnect material.¹⁷ Its low dimensionality, flexibility and re-workability made it an interesting material to research in what some described as a “gold rush” of research. A decade and a half later the discovery of its exceptional thermal properties^{18–22} and with development of new techniques for cost effective mass production of few layer graphene (FLG) flakes, thermal management of electronics became the most feasible of graphene’s industrial application. Large sums of research has been conducted showing its use in composites, thermal interface materials, and other thermal packaging related material systemsa.^{23–31} All of these efforts have predominantly focused on epoxy based thermal composites, which also have many applications in electronics as well.^{25,29–32}

1.2 Historical Perspective

Electronic packaging can be summed into the five distinct eras of processing technology,^{33,34} each ending with the introduction of new technological advancements. Figure 1.1 shows a timeline of electronic and packaging history through the past half-century. From the early vacuum tube computers to more recent micro-processors thermal energy has always been a bi-product of electronic increasing processing speed. The earliest vacuum tube computer systems such as the ENIAC³⁵ (electronic numerical integrator and computer) had strict room temperatures as well as moisture limits which were kept at around 20°C to 25°C,³⁴ these parameters were simple and sufficient in keeping systems

running by removing the warm air from the room and replacing it with cool air. Seeing as this was sufficient for these large mainframes few questions were asked as about the source of the thermal energy. As chip technology changed and the introduction of transistors,³⁶ followed by the integrated circuit,³⁷ then microprocessors³⁸ were made, changes to the cooling systems had to be made, now these large mainframes incorporated a semi-directional use of air or liquid to keep the computers cool.

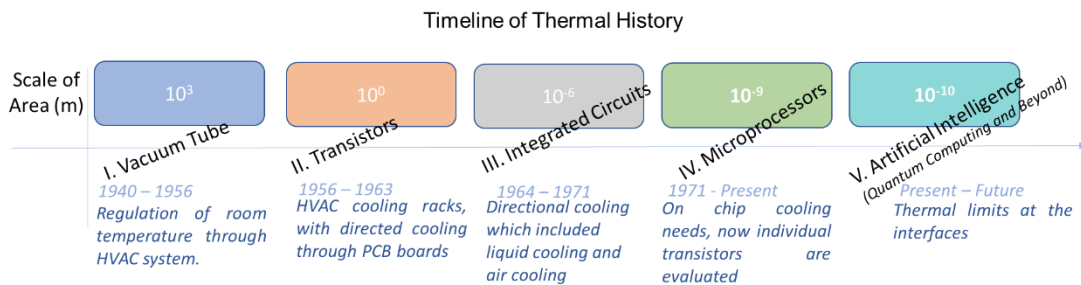


Figure 1.1: A historical timeline of the five eras of processing power. As technological advancements were made and the chip density increased, the ways of removing thermal energy became more and more complex, with the dimensions to which monitoring of thermal dissipation decreases in size.

In the early 1980’s, despite the opposition of many directives, and liquid and refrigerated cooling systems were used for a long period of time. In the late 1980’s with advancements in microprocessors and the further increase in chip density, more attention had to be paid to the individual components which were generating heat.^{34,39} The interfaces which were once overlooked had to be carefully examined and new “cooling plate” methods (heat sinks) were used, with this came the use of thermal interface materials (TIMs), which were very monumental in keeping a continuous flow of heat out of the system. When the use of the cooling plate began, a thin layer of oil was placed in the interface of the two surfaces to reduce the contact resistance, followed by the addition of

thermally conductive fillers later on. The focus on interfacial dynamics and the use of TIMs has continued the technological momentum which we see today. This technology of using TIMs to continuously move heat from one interface to another has aided in the development of new technologies. Now approaching the beginning of what is described as the 5th generation of computing power, the need for better removal of heat will be the bottleneck.⁴⁰⁻⁴² This work addresses the overall need for better performing noncuring TIMs. Historical overview and overall perspective show that in the coming years current methods to cool electronics will no longer be viable. An approach to aid is through the improvement of thermal transport and mechanical properties of TIMs *via* the addition of novel two-dimensional highly conductive filler as graphene and investigation of techniques which create robust TIMs using this exotic material.

References

1. Zanella, A., Bui, N., Castellani, A., Vangelista, L. & Zorzi, M. Internet of Things for Smart Cities. *IEEE Internet of Things Journal* **1**, 22–32 (2014).
2. Islam, S. M. R., Kwak, D., Kabir, M. H., Hossain, M. & Kwak, K. S. The Internet of Things for Health Care: A Comprehensive Survey. *IEEE Access* **3**, 678–708 (2015).
3. Militano, L., Araniti, G., Condoluci, M., Farris, I. & Iera, A. Device-to-Device Communications for 5G Internet of Things. *EAI Endorsed Transactions on Internet of Things* **1**, 150598 (2015).
4. Mahajan, R., Chiu, C. & Chrysler, G. Cooling a Microprocessor Chip. *Proceedings of the IEEE* **94**, 1476–1486 (2006).
5. Ma, H., Yu, D. & Wang, J. The Development of Effective Model for Thermal Conduction Analysis for 2.5D Packaging Using TSV Interposer. in *Microelectronics Reliability* **54**, 425–434 (2014).
6. Loeblein, M., Tsang, S. H., Han, Y., Zhang, X. & Teo, E. H. T. Heat Dissipation Enhancement of 2.5D Package with 3D Graphene and 3D Boron Nitride Networks as Thermal Interface Material (TIM). in *Proceedings - Electronic Components and Technology Conference 2016-August*, 707–713 (Institute of Electrical and Electronics Engineers Inc., 2016).
7. Moore, G. E. Cramming More Components Onto Integrated Circuits, Reprinted from *Electronics*, volume 38, number 8, April 19, 1965, pp.114 ff. *IEEE Solid-State Circuits Society Newsletter* **11**, 33–35 (2006).
8. Moore, A. L. & Shi, L. Emerging Challenges and Materials for Thermal Management of Electronics. *Materials Today* **17**, 163–174 (2014).
9. Pop, E., Sinha, S. & Goodson, K. E. Heat Generation and Transport in Nanometer-Scale Transistors. *Proceedings of the IEEE* **94**, 1587–1601 (2006).
10. Otiaba, K. C., Ekere, N. N., Bhatti, R. S., Mallik, S., Alam, M. O. & Amalu, E. H. Thermal Interface Materials for Automotive Electronic Control Unit: Trends, Technology and R&D Challenges. *Microelectronics Reliability* **51**, 2031–2043 (2011).
11. Mallik, S., Ekere, N., Best, C. & Bhatti, R. Investigation of Thermal Management Materials for Automotive Electronic Control Units. *Applied Thermal Engineering* **31**, 355–362 (2011).

12. 'Tsunami of data' could consume one fifth of global electricity by 2025 | Environment | The Guardian. at <https://www.theguardian.com/environment/2017/dec/11/tsunami-of-data-could-consume-fifth-global-electricity-by-2025>
13. Novoselov, K. S., Geim, A. K., Morozov, S. V, Jiang, D., Zhang, Y., Dubonos, S. V, Grigorieva, I. V & Firsov, A. A. Electric Field Effect in Atomically Thin Carbon Films. *Science* **306**, 666–9 (2004).
14. Geim, A. K. & Novoselov, K. S. The Rise of Graphene. *Nature Materials* **6**, 183–191 (2007).
15. Schwierz, F. Graphene Transistors. *Nature Nanotechnology* **5**, 487–496 (2010).
16. Hernandez, Y., Nicolosi, V., Lotya, M., Blighe, F. M., Sun, Z., De, S., McGovern, I. T., Holland, B., Byrne, M., Gun'Ko, Y. K., Boland, J. J., Niraj, P., Duesberg, G., Krishnamurthy, S., Goodhue, R., Hutchison, J., Scardaci, V., Ferrari, A. C. & Coleman, J. N. High-yield Production of Graphene by Liquid-Phase Exfoliation of Graphite. *Nature Nanotechnology* **3**, 563–568 (2008).
17. Shao, Q., Liu, G., Teweldebrhan, D. & Balandin, A. A. Higherature Quenching of Electrical Resistance in Graphene Interconnects. *Applied Physics Letters* **92**, (2008).
18. Balandin, A. A., Ghosh, S., Bao, W., Calizo, I., Teweldebrhan, D., Miao, F. & Lau, C. N. Superior Thermal Conductivity of Single-Layer Graphene. *Nano Letters* **8**, 902–907 (2008).
19. Balandin, A. A. Thermal Properties of Graphene and Nanostructured Carbon Materials. *Nature Materials* **10**, 569–581 (2011).
20. Shahil, K. M. F. & Balandin, A. A. Thermal Properties of Graphene and Multilayer Graphene: Applications in Thermal Interface Materials. *Solid State Communications* **152**, 1331–1340 (2012).
21. Nika, D. L., Pokatilov, E. P., Askerov, A. S. & Balandin, A. A. Phonon Thermal Conduction in Graphene: Role of Umklapp and Edge Roughness Scattering. *Physical Review B - Condensed Matter and Materials Physics* **79**, 155413 (2009).
22. Fugallo, G., Cepellotti, A., Paulatto, L., Lazzeri, M., Marzari, N. & Mauri, F. Thermal Conductivity of Graphene and Graphite: Collective Excitations and Mean Free Paths. *Nano Letters* **14**, 6109–6114 (2014).
23. Goyal, V. & Balandin, A. A. Thermal Properties of the Hybrid Graphene-Metal Nano-Micro-Composites: Applications in Thermal Interface Materials. *Applied Physics Letters* **100**, 073113 (2012).

24. Goli, P., Legedza, S., Dhar, A., Salgado, R., Renteria, J. & Balandin, A. A. Graphene-enhanced Hybrid Phase Change Materials for Thermal Management of Li-ion Batteries. *Journal of Power Sources* **248**, 37–43 (2014).
25. Kargar, F., Barani, Z., Salgado, R., Debnath, B., Lewis, J. S., Aytan, E., Lake, R. K. & Balandin, A. A. Thermal Percolation Threshold and Thermal Properties of Composites with High Loading of Graphene and Boron Nitride Fillers. *ACS Applied Materials & Interfaces* **10**, 37555–37565 (2018).
26. Song, S. H., Park, K. H., Kim, B. H., Choi, Y. W., Jun, G. H., Lee, D. J., Kong, B.-S., Paik, K.-W. & Jeon, S. Enhanced Thermal Conductivity of Epoxy-Graphene Composites by Using Non-Oxidized Graphene Flakes with Non-Covalent Functionalization. *Advanced Materials* **25**, 732–737 (2013).
27. Phuong, M.T.; Trinh, P.V.; Tuyen, N.V.; Dinh, N.N.; Minh, P.N.; Dung, N.D.; Thang, B. H. Effect of Graphene Nanoplatelet Concentration on the Thermal Conductivity of Silicone Thermal Grease. *Physics, Journal of Nano- and Electronic* **11**, 5039 (2019).
28. Ma, W., Yang, F., Shi, J., Wang, F., Zhang, Z. & Wang, S. Silicone Based Nanofluids Containing Functionalized Graphene Nanosheets. *Colloids and Surfaces A: Physicochemical and Engineering Aspects* **431**, 120–126 (2013).
29. Lewis, J. S., Barani, Z., Magana, A. S., Kargar, F. & Balandin, A. A. Thermal and Electrical Conductivity Control in Hybrid Composites with Graphene and Boron Nitride Fillers. *Materials Research Express* **6**, (2019).
30. Yu, A., Ramesh, P., Itkis, M. E., Bekyarova, E. & Haddon, R. C. Graphite Nanoplatelet-Epoxy Composite Thermal Interface Materials. *Journal of Physical Chemistry C* **111**, 7565–7569 (2007).
31. Kargar, F., Salgado, R., Legedza, S., Renteria, J. & Balandin, A. A. A Comparative Study of The Thermal Interface Materials with Graphene and Boron Nitride Fillers. in *Carbon Nanotubes, Graphene, and Associated Devices VII* **9168**, 91680S (SPIE, 2014).
32. Li, Q., Guo, Y., Li, W., Qiu, S., Zhu, C., Wei, X., Chen, M., Liu, C., Liao, S., Gong, Y., Mishra, A. K. & Liu, L. Ultrahigh Thermal Conductivity of Assembled Aligned Multilayer Graphene/Epoxy Composite. *Chemistry of Materials* **26**, 4459–4465 (2014).
33. Smoyer, J. L. & Norris, P. M. Brief Historical Perspective in Thermal Management and the Shift Toward Management at the Nanoscale. *Heat Transfer Engineering* **40**, 269–282 (2019).

34. Avram, B. Encyclopedia Of Thermal Packaging, Set 2: Thermal Packaging Tools (A 4-volume Set). (2014).
35. Jr., T. R. K. Electronic Computer Flashes Answers, May Speed Engineering. *The New York Times* (1946).
36. Bardeen, J. & Brattain, W. H. The Transistor, A Semi-Conductor Triode. *Physical Review* **74**, 230–231 (1948).
37. Kilby, J. S. Invention of the Integrated Circuit. *IEEE Transactions on Electron Devices* **23**, 648–654 (1976).
38. Sack, E. A., Lyman, R. C. & Chang, G. Y. Evolution of the Concept of a Computer on a Slice. *Proceedings of the IEEE* **52**, 1713–1720 (1964).
39. Mahajan, R., Chiu, C. P. & Chrysler, G. Cooling a Microprocessor Chip. *Proceedings of the IEEE* **94**, 1476–1485 (2006).
40. Almudever, C. G., Lao, L., Fu, X., Khammassi, N., Ashraf, I., Iorga, D., Varsamopoulos, S., Eichler, C., Wallraff, A., Geck, L., Kruth, A., Knoch, J., Bluhm, H. & Bertels, K. The Engineering Challenges in Quantum Computing. in *Proceedings of the 2017 Design, Automation and Test in Europe* 836–845 (IEEE, 2017). doi:10.23919/DATE.2017.7927104
41. Pros vs. Cons of Implementing IoT Programs in Your Facility - Therma. at <<https://www.therma.com/pros-vs-cons-of-implementing-iot-programs-in-your-facility/>>
42. 5G Modems and Phones Literally Can't Handle the Heat of Summer Weather - ExtremeTech. at <<https://www.extremetech.com/mobile/295228-5g-modems-and-phones-literally-cant-handle-the-heat-of-summer-weather>>

Chapter 2: Phonons, Thermal Conductivity and Thermal Management

2.1 Introduction

As we approach fundamental limits, individual devices contain only thousands of surface atoms—a scale at which bulk materials lose their properties.¹ The latter is associated with a large range of challenges ranging from thermal management to novel fabrication paradigms. How to provide high-quality electronics that meet thermal budgets, as well as low power consumption are the fuel for this work. The drive for smaller and faster devices has led many to describe thermal limits as an inevitable problem needing to be addressed. The International Technology Roadmap for Semiconductors (ITRS)² has stressed the need for new technology to manage heat including dynamic materials that are capable of sustaining non-uniform heat transfer throughout the device, water cooled systems as well as algorithmic solutions which would use the components more efficiently.² All electronic components today are thermally limited whether in processing or functionality. The lack of models to base heat transfer from one interface to another has made accurate predictions of thermal dissipation difficult.

This work focuses on the study and development of thermal interface materials as well as the limitations associated with development and an overview of the current state of the art. TIMs are a unique group of composites used to fill void gaps created at the interface of two uneven surfaces. Their function is to fill in the voids and reduce thermal resistance

cause by air. Typically, they are made of a polymer base with fillers dispersed throughout, the fillers are the main carrier of thermal energy in this system.

2.2 Graphene

The successful separation of a single sheet of graphene from bulk graphite set the pace for a new field of research. The strong in-plane bonding and weak out-of-plane Van der Waals forces, make it possible to separate this material sheet by sheet.^{3,4} At only an atom thick it has many exotic properties including large carrier mobility, high thermal conductivity, it is nearly transparent and one of the strongest materials ever measured.⁴⁻⁶ Graphene is a single layer van der Waals material bonded by sp^2 hybridized carbons arranged in a honeycomb lattice. Theorized for half a century to be unstable in a few-layer state. Thermodynamic constraints and difficulty separating each layer many thought it was unstable below a given thickness.

The discovery of graphene's unique heat conduction properties⁶⁻¹⁰ motivated numerous practically oriented studies on the use of graphene and few-layer graphene (FLG) in various composites, thermal interface materials and coatings.^{8,11-17} Thermal enhancement is strong with composites where graphene is used as the filler base. The thermal conductivity of a sample with 45% filler content reaches as high as $12 \text{ Wm}^{-1}\text{K}^{-1}$.¹⁸ Although epoxy based TIMs show excellent potential for various applications, the hardening process of epoxy makes them unsuitable for use in commercial electronics, where a soft noncuring TIM is preferred. There are a few papers where graphene is incorporated into commercial TIMs, enhancing the thermal conductivity of the commercially available products.⁸ Although it showed improvement it does not give a clear

understanding of the interaction between graphene and the base TIM used. Our approach uses a simple model with few steps and known materials. The obtained results exceed industry metrics giving a simple effective model on the interaction of graphene and its base material.

2.3 Thermal Management

The continuous miniaturization of electronic components shows promise in increased processing power and speed. A byproduct of the increase in processing power and speed is an increase in the heat dissipated from the created devices. Household and everyday common items are continuously connected to Wi-Fi networks and automated, the market with the quickest growth outside of electronic components outside of mobile phones and computers, is the automotive electronic industry.^{19,20} The ever increasing complexity in devices applications has led development of electronics with new condition ranges, including temperatures and functionals. This further complicates many components inside of the vehicle ranging from new rechargeable batteries to electronic lifetimes. The advent of autonomous vehicles (AV) and electric vehicles (EV) has made the electronics within cars more complex as well, including various sensors in the exterior portions of the automobile, interior computer and touch display for facile changes and continuous monitoring of vehicle status, and the large Li-ion batteries which tend to be temperature dependent.^{19,20} Figure 2.1 displays the various markets and industries affected by thermal limitations, including electric vehicles, medical devices, computers and handhelds, telecommunication and solar energy. The need for higher performing thermal interface materials are and will continue to be a necessity for continuous innovation in these fields.

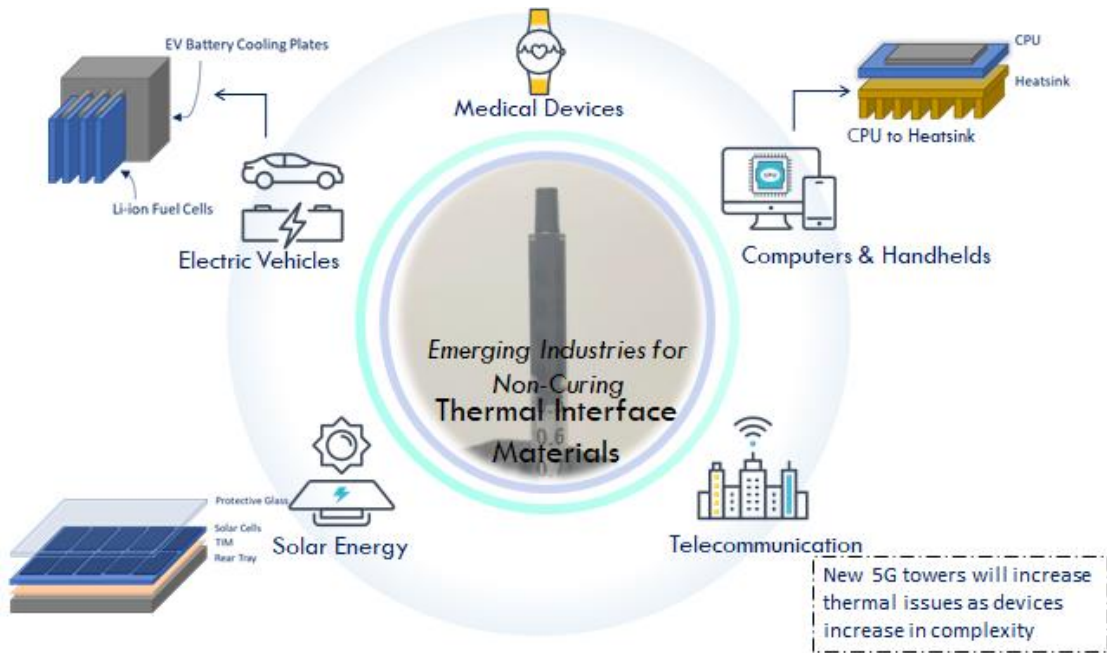


Figure 2.1: The various industries which are dependent on advancements in TIMs. (Clockwise from top) Medical devices and wearables, computers and handhelds, telecommunication, solar panel advancement and electric vehicles.

For the last quarter century heat sinks and fans have been one of the primary ways to cool electronic components. Heat sinks are large pieces of metal with riveted fins for optimal surface area for cooling, they tend to be made from materials with high thermal conductivity such as copper alloys and aluminum.²¹ These heatsinks are bound to the chip using a TIM, which fills in the air gaps and improves the flow of heat from one interface into the other, shown in Figure 2.2. The thermal resistance retained at interface junctions such as the one just described is the make or break for the electronics function as a whole, overheating being the other option.

2.4 Phonons and Thermal Conductivity

Thermal Conductivity (k) is an inherent material property, describing the rate at which heat moves through a material or material system. Fourier's Law describes heat flux (q) as the product of the thermal conductivity (k) and the gradient temperature (∇T) in one direction, thermal conductivity is the constant material property. The units for thermal conductivity are $[\text{Wm}^{-1}\text{K}^{-1}]$.²²

$$q'' = k \frac{\Delta T}{\Delta x} \quad (2.1)$$

There are two methods which thermal energy can move through a material either with electrons, phonons, or both. Metals tend to propagate thermal energy predominantly with free electrons. The thermal conductivity of non-metal materials such as semiconductors is a sum of both the thermal conductivity contribution from electrons (K_e) and phonons (K_p).

$$k = k_e + k_p \quad (2.2)$$

The Drude model was used to explain the empirical law Weidemann-Franz law, which describes a relationship between electrical conductivity (σ) and thermal conductivity (K) and their direct dependence to temperature (T) in metals. Drude's model assumes that most of the thermal energy is carried by the electrons which fits fairly precisely as an approximation for the thermal conductivity of metals, as shown below.

$$\frac{k_e}{\sigma T} = \frac{\pi^2 k_B^2}{3e^2} \quad (2.3)$$

Other non-metal materials conduct heat primarily *via* acoustic phonons. Phonons are quasi particles which describe the vibrational modes of a material. Their energy and momentum are described below as:

$$E = \hbar\omega \quad (2.4)$$

$$P = \hbar k \quad (2.5)$$

Acoustic phonons are the predominant carrier of heat in many non-metallic solid systems. The formula below presents an estimate of phonon contribution to the thermal conductivity of a system.

$$k_p = \frac{1}{3} C_v v_p \lambda_p \quad (2.6)$$

In this equation, C_v is the volumetric heat capacity, v_p is the phonon group velocity, and λ_p is the phonon mean free path (MFP), respectively.

2.5 Thermal Interface Materials

Thermal interface materials are a group of materials commonly overlooked in the everyday setting. They are materials which bind two uneven surfaces and aid in the removal of heat, by reducing the thermal resistance, described in Figure 2.2. They are generally comprised of a base material, usually a polymer, conveniently filled with micron-scale fillers. These fillers define the TIM and its desired function, whether being electrically insulating, conducting or thermally insulating or conducting. TIMs have three predominant categories: *curing*, *noncuring* and *phase change materials (PCM)*. *Curing* TIMs are those which are solid or dry to a solid and are used as adhesives. They include pads, tapes and other pastes which dry to a solid, many tend to be epoxy based. *Noncuring* TIMs are soft materials which are easy to apply and paste-like. The most common are thermal greases they are used to bind the interface of many electronic components and are commonly used for the interface of a CPU to heat sink. *PCMs* are wax like materials which change phase as they absorb or release heat and have many applications in electric vehicles and battery cooling.

Figure 2.3 is a schematic differentiating between the three types as well as their applications.

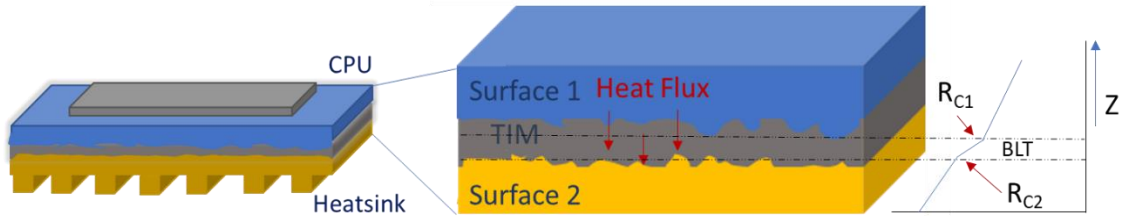


Figure 2.2: Thermal interface materials are at the center of thermal management of most electronics, they bind two uneven surfaces, such as a die and heat sink (shown above). They reduce thermal resistance between the two uneven surfaces which they bind.

This work focuses primarily on *noncuring* TIMs, commonly known as thermal compounds or thermal greases. Noncuring TIMs comprise of particle-laden grease, either silicone or carbon based and are historically difficult to synthesize. They were first used in the late 1970's when only attaching a cooling plate to die component was not enough to maintain optimum computer working temperatures.²¹ The uneven surface contact between the components was identified as the limitation, where the grease was used to fill the voids. Unlike curing TIMs which dry to a solid, noncuring TIMs are easier to use. In electronic applications where heat fluctuations are constant, curing TIMs are limited by contrasting thermal expansion coefficient between them and the component causing mechanical instability cracking in the TIM layer making them unideal.

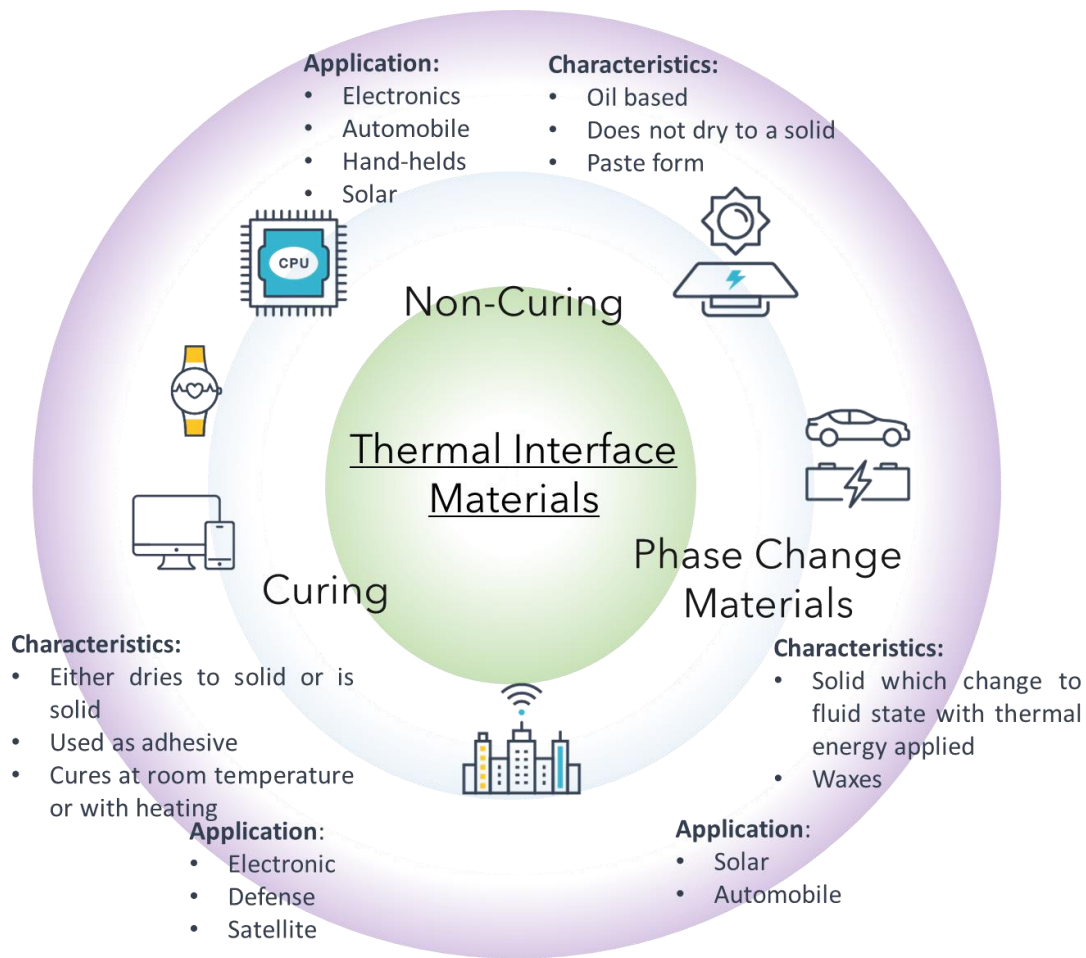


Figure 2.3: Subgroups of thermal interface materials which include *noncuring*, *phase change materials*, and *curing* (clockwise). Applications for TIMs continues to grow and includes automobiles, consumer electronics and wearables.

Electronics today have various TIM layers within them. TIMs are one of the primary modes of heat removal in electronic device. They are most commonly used to bind the interface of heat sinks to chips, as well as the cooling for electric batteries and solar cell cooling. Critical to a TIMs success is the filler chosen. Fillers have many properties which must be accounted for before chosen, the first being their inherent thermal conductivity. Most of the thermal properties of a TIM arises from the fillers incorporated

into the matrix. Generally, the higher the thermal conductivity the higher the likelihood a TIM will perform well. Although straight forward in concept this becomes increasingly difficult when factoring in the effects which processing has on the filler will have on the effect of the filler and the overall TIM. properties. Of the various materials that have been heavily researched and used the most promising for thermal applications is graphene, a two-dimensional material with exceptionally high thermal conductivity and electrical conductivity.^{3,4,13,23,24}

2.6 Summary

The increase in chips density and demand for high power electronics has exceeded the current thermal budget on various electronic platforms, both in-chip and on-chip. Various scientific outlets have stressed the need for better management systems for excess heat produced. Heat dissipation through a material is defined by its thermal conductivity, produced by either phonons or electrons. The thermal energy (heat) is generated through the vibration and excitation of electrons and phonons, which each individually donates to the overall thermal conductivity, as previously described. To help with heat removal various electronics contains thin materials called TIMs, they fill the air gaps in between two uneven interfaces, improving heat transfer and overall device performance. TIMs are generally comprised of polymer bases with very low thermal conductivity laden with highly conductive fillers dispersed throughout. The most promising filler which is readily available and has exceptional thermal properties is graphene, a two-dimensional material.

References

1. Moore, G. E. Cramming More Components Onto Integrated Circuits, Reprinted from Electronics, volume 38, number 8, April 19, 1965, pp.114 ff. *IEEE Solid-State Circuits Society Newsletter* **11**, 33–35 (2006).
2. 2015 International Technology Roadmap for Semiconductors (ITRS) - Semiconductor Industry Association. at <https://www.semiconductors.org/resources/2015-international-technology-roadmap-for-semiconductors-itrs/>
3. Novoselov, K. S., Geim, A. K., Morozov, S. V, Jiang, D., Zhang, Y., Dubonos, S. V, Grigorieva, I. V & Firsov, A. A. Electric Field Effect in Atomically Thin Carbon Films. *Science* **306**, 666–9 (2004).
4. Geim, A. K. & Novoselov, K. S. The Rise of Graphene. *Nature Materials* **6**, 183–191 (2007).
5. Novoselov, K. S., Geim, A. K., Morozov, S. V, Jiang, D., Zhang, Y., Dubonos, S. V, Grigorieva, I. V & Firsov, A. A. Electric Field Effect in Atomically Thin Carbon Films. *Science* **306**, 666 LP – 669 (2004).
6. Balandin, A. A. Thermal Properties of Graphene and Nanostructured Carbon Materials. *Nature Materials* **10**, 569–581 (2011).
7. Ghosh, S., Calizo, I., Teweldebrhan, D., Pokatilov, E. P., Nika, D. L., Balandin, A. A., Bao, W., Miao, F. & Lau, C. N. Extremely High Thermal Conductivity of Graphene: Prospects for Thermal Management Applications in Nanoelectronic Circuits. *Applied Physics Letters* **92**, 151911 (2008).
8. Renteria, J., Legedza, S., Salgado, R., Balandin, M. P., Ramirez, S., Saadah, M., Kargar, F. & Balandin, A. A. Magnetically-Functionalized Self-Aligning Graphene Fillers for High-Efficiency Thermal Management Applications. *Materials and Design* **88**, 214–221 (2015).
9. Jauregui, L. A., Yue, Y., Sidorov, A. N., Hu, J., Yu, Q., Lopez, G., Jalilian, R., Benjamin, D. K., Delk, D. A., Wu, W., Liu, Z., Wang, X., Jiang, Z., Ruan, X., Bao, J., Pei, S. S. & Chen, Y. P. Thermal Transport in Graphene Nanostructures: Experiments and Simulations. in *ECS Transactions* **28**, 73–83 (2010).
10. Cai, W., Moore, A. L., Zhu, Y., Li, X., Chen, S., Shi, L. & Ruoff, R. S. Thermal Transport in Suspended and Supported Monolayer Graphene Grown by Chemical Vapor Deposition. *Nano Letters* **10**, 1645–1651 (2010).
11. Yan, Z., Liu, G., Khan, J. M. & Balandin, A. A. Graphene Quilts for Thermal

- Management of High-Power GaN Transistors. *Nature Communications* **3**, 827 (2012).
12. Shahil, K. M. F. & Balandin, A. A. Graphene–Multilayer Graphene Nanocomposites as Highly Efficient Thermal Interface Materials. *Nano Letters* **12**, 861–867 (2012).
 13. Shahil, K. M. F. & Balandin, A. A. Thermal Properties of Graphene and Multilayer Graphene: Applications in Thermal Interface Materials. *Solid State Communications* **152**, 1331–1340 (2012).
 14. Goli, P., Ning, H., Li, X., Lu, C. Y., Novoselov, K. S. & Balandin, A. A. Thermal Properties of Graphene–Copper–Graphene Heterogeneous Films. *Nano Letters* **14**, 1497–1503 (2014).
 15. Goli, P., Legedza, S., Dhar, A., Salgado, R., Renteria, J. & Balandin, A. A. Graphene-enhanced Hybrid Phase Change Materials for Thermal Management of Li-ion Batteries. *Journal of Power Sources* **248**, 37–43 (2014).
 16. Saadah, M., Gamalath, D., Hernandez, E. & Balandin, A. A. Graphene-Enhanced Thermal Interface Materials for Heat Removal from Photovoltaic Solar Cells. in (eds. Razeghi, M., Ghazinejad, M., Bayram, C. & Yu, J. S.) **9932**, 99320H (International Society for Optics and Photonics, 2016).
 17. Kargar, F., Salgado, R., Legedza, S., Renteria, J. & Balandin, A. A. A Comparative Study of The Thermal Interface Materials with Graphene and Boron Nitride Fillers. in **9168**, 91680S (SPIE, 2014).
 18. Kargar, F., Barani, Z., Salgado, R., Debnath, B., Lewis, J. S., Aytan, E., Lake, R. K. & Balandin, A. A. Thermal Percolation Threshold and Thermal Properties of Composites with High Loading of Graphene and Boron Nitride Fillers. *ACS Applied Materials & Interfaces* **10**, 37555–37565 (2018).
 19. Otiaba, K. C., Ekere, N. N., Bhatti, R. S., Mallik, S., Alam, M. O. & Amalu, E. H. Thermal Interface Materials for Automotive Electronic Control Unit: Trends, Technology and R&D Challenges. *Microelectronics Reliability* **51**, 2031–2043 (2011).
 20. Mallik, S., Ekere, N., Best, C. & Bhatti, R. Investigation of Thermal Management Materials for Automotive Electronic Control Units. *Applied Thermal Engineering* **31**, 355–362 (2011).
 21. Avram, B. Encyclopedia Of Thermal Packaging, Set 2: Thermal Packaging Tools (A 4-volume Set). (2014).

22. Characteristics of Thermal Interface Materials. 1–6 (2001).
23. Balandin, A. A., Ghosh, S., Bao, W., Calizo, I., Teweldebrhan, D., Miao, F. & Lau, C. N. Superior Thermal Conductivity of Single-Layer Graphene. *Nano Letters* **8**, 902–907 (2008).
24. Calizo, I., Balandin, A. A., Bao, W., Miao, F. & Lau, C. N. Temperature Dependence of the Raman Spectra of Graphene and Graphene Multilayers. *Nano Letters* **7**, 2645–2649 (2007).

Chapter 3: Sample Preparation and Thermal Conductivity Measurement Tools

3.1 Introduction

There are various techniques used to characterize the many properties of TIMs. The techniques used in this investigation were to determine mechanical and thermal properties as well as characterize the effects which sample preparation has on the noncuring TIM. In this work a steady state thermal impedance measurement method was used to extract the thermal conductivity. The instrumentation included a steady state TIM tester to measure thermal impedance, scanning electron microscope (SEM), Raman spectrometer, as well as a rheometer.

3.2 Steady State Thermal Conductivity Measurement Method

The steady state method also known as a TIM tester is an established method used to characterize the thermal properties of materials. It follows the guidelines set forth by the ASTM D5470. In this method, a sample is placed between two interfaces, one interface being the heating source, the other interface observes the temperature drop, from which thermal resistance is extracted. The through-plane thermal impedance measurements of our graphene based TIMs were measured at 303 K (30°C) with a LW-9389 TIM Tester (LonGwin, Taiwan) (Figure 3.1) utilizing the steady-state heat flow technique prescribed in the ASTM D5470.¹ The experimental setup is quite simple it consists of two parallel thermally isolated steel plates, one plate with an elevated temperature and the other cooled. The sample is then placed in between these two plates and measurements can take place. The extracted data is based on the surface temperature difference at the two interfaces.

Thermal conductivity (k) was extracted from thermal resistance measurements at constant applied pressure with varying thicknesses. The LonGwin TIM tester used for these experiments is equipped with six precision thermocouples positioned in both the heating and cooling blocks along the direction of the thermal gradient. These measurements are conducted using 4 to 6 uniform thicknesses of the thermal pastes (0.1 to 1 mm).

3.2.1 Theory of the Steady State Method

The TIM tester measures thermal resistance across a sample which is placed between the two parallel plates. Thermal resistance is the temperature gradient per unit of thermal flux, passing through the sample and being measured. While measuring, the sample is placed between the two plates with careful attention paid to soft samples while measuring, making sure that they sample does not expand or spread outside of the boundaries within the two plates. Once the sample is spread onto the lower bar (heating block) the upper bar (cooling block) is slowly down onto the sample with zero applied pressure. Equation 3.1 shows the calculations for heat flux using this set up.

When measuring thermal impedance of the sample simple principles are used in the calculation. The heat flux calculation below relates to Figure 3.2 in showing which thermometers are used to measure the flux. ΔX is the distance between T_L and T_u , A is the surface area of the sample plates, and k_m is the meter bars thermal conductivity. Total heat flux, q'' , is the average of the heat flux from both the cooling plate, q''_c and q''_h .

$$q''_h = k_m A \cdot \nabla T \quad (3.1)$$

$$q''_h = k_m A \cdot \frac{T_l - T_u}{\Delta X} \quad (3.2)$$

$$q''_h = k_m A \cdot \frac{T_{l1} - T_{l3}}{\Delta X} \quad (3.3)$$

$$q'' = \frac{Q_h + Q_c}{2} \quad (3.3)$$

The thermal resistance within the instruments' software uses the value obtained from heat flux above and is the difference in temperature of the cold plate surface to the hot plate surface divided by the heat flux, shown below (3.5). Similarly, impedance is the resistance multiplied by the area and has the units of $\text{Kcm}^2\text{W}^{-1}$.

$$R'' = \frac{T_c - T_d}{Q} \quad (3.5)$$

Data points are then plotted to extract the thermal conductivity. From these plots we were also able to extract contact resistance, the y – intercept of our data. The instrument water cooling system was kept at a constant temperature of 298 K (25°C) throughout all experiments and no pressure was applied unless specifically stated.



Figure 3.1: TIM tester (LonGwin) used to conduct all thermal measurements for noncuring thermal interface materials used. This instrument allows for various aspects to be controlled while measuring including pressure, temperature control of measurements. Nanofabrication Facility, UC Riverside, 2019.

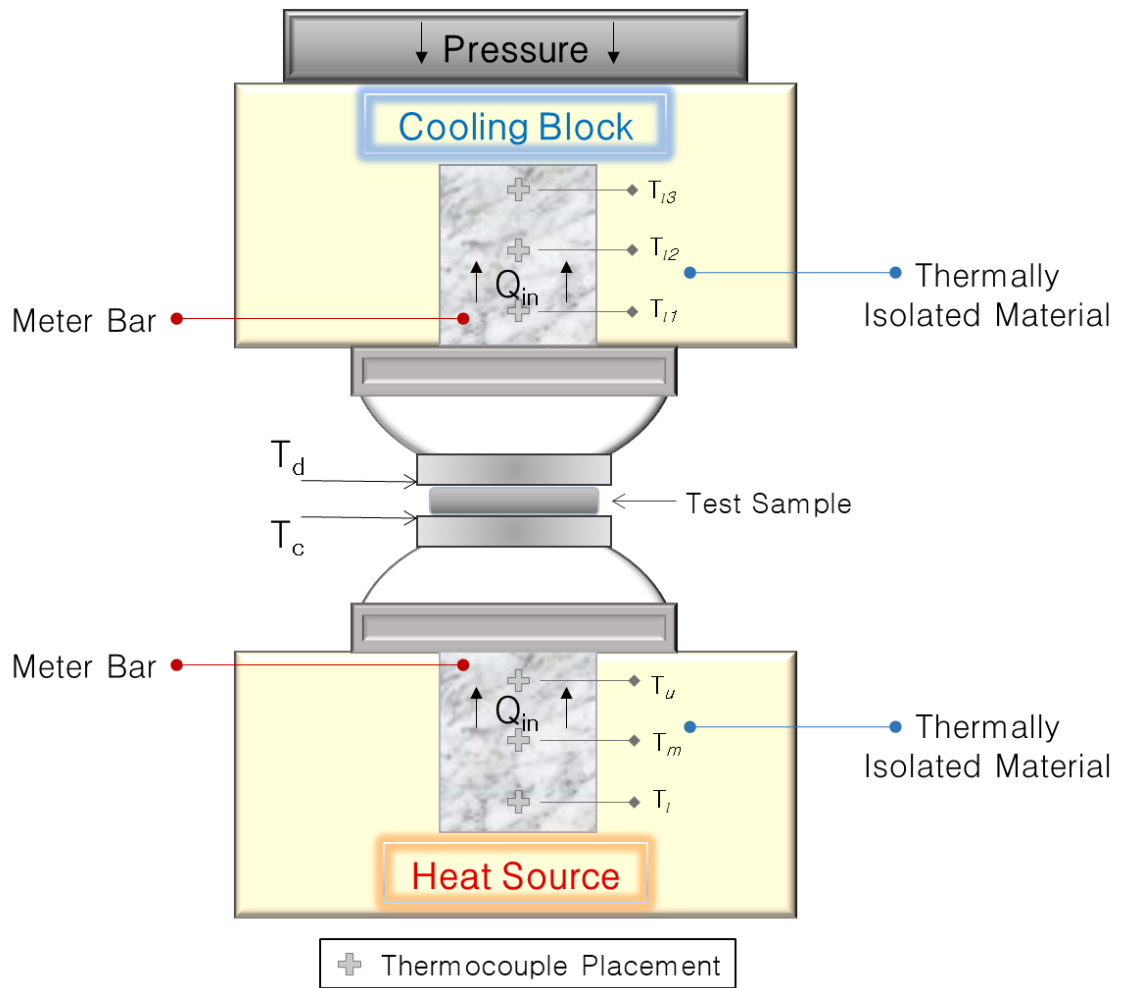


Figure 3.2: Schematic of TIM tester (LonGwin). A sample is placed in between two plates labeled T_d and T_c and measured at varying thicknesses. Standard steady state ASTM testing setup.

Once the noncuring TIM is prepared the sample is evenly spread onto the lower bar of our TIM tester. The upper bar is then lowered slowly down onto the sample, at zero pressure. The instrument is ready to measure the sample. The instrument software allows for temperature and pressure dependent measurements respectively and concurrently. For the purposes of this work, we measured both parameters separately. Before each measurement there is a delay of 1800 seconds allowing for the system to reach a steady state condition where the impedance and temperature are both stable.

3.3 Sample Preparation

Homogenous dispersion of fillers within the TIM is important to the integrity of the measurements taken as well as the TIMs functionality. In this work, the samples were prepared using commercially produced graphene flakes (XG Sciences) with lateral dimension around $\sim 25 \mu\text{m}$. The thickness varied from single atomic planes of 0.35 nm to ~ 12 nm. The graphene mixtures were not optimized for achieving the largest thermal conductivity enhancement.^{10,11} The materials were used as is and created high performing TIMs. In a typical experiment, around 3 grams of mineral oil is added to container, next a predetermined amount of graphene is weighed out based on the total weight fraction of the TIM. We ensure proper dispersion of the graphene by then adding in about twice the weight of graphene and mineral oil mix, in acetone. Next the samples are mixed using a high-speed shear mixer (Flacktek Inc.) at the lowest possible mixing rates of 310 rpm for 20 minutes. This step binds the graphene and mineral oil while separating them from the acetone. Finally, the mixture is placed in an oven for ~ 2 hours at 343 K (70° C) to remove any remaining acetone. This process yields a smooth paste that is easily spreadable and homogenous.

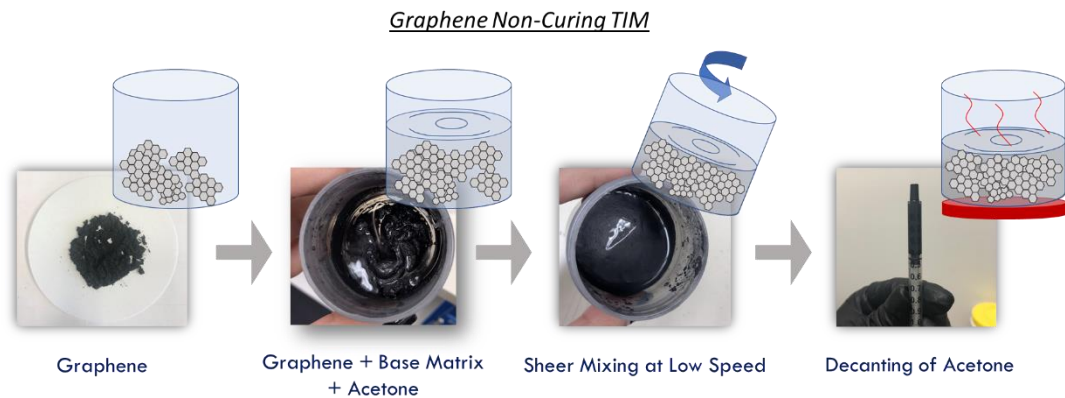


Figure 3.3: Process flow of sample preparation for noncuring graphene TIMs.

When developing the procedure for producing the noncuring TIM, various techniques were evaluated for sample preparation ranging from varying rate of sheer mixing, sonication as well as different graphene flake sizes. Three parameters were identified as determining factors affecting the TIMs thermal conductivity. First, the rate of mixing was evaluated looking at samples with constant a loading fraction and solely change the rate of mixing. Second, we evaluated the effects which the graphene flakes dimension had on the TIM. Table 3.1 shows the varying parameters and optimization with each changing parameter.

Spin speed was the first optimized parameter. The recent development of graphene liquid exfoliation has expanded the availability and versatility through various chemical and mechanical treatments, tuning of the graphene flake is possible, there-by tuning thermal conductivity of the samples by varying the mixing speed which controls the overall lateral dimensions.² We wanted to tune our parameters so that the properties of the graphene flakes would be kept intact, keeping our flake size and not further breaking them down. Our first samples were mixed using the above-mentioned steps, but initially with a

higher mixing speed of 2500 rpm. This sample yielded a thermal conductivity of $1 \text{ Wm}^{-1}\text{K}^{-1}$. We determined the higher the spin speed, the lower the thermal conductivity we obtained for the TIM at constant filler loading compared to samples similarly prepared with a lower spin speed. Mehrali et al³ summarizes the effects that higher mixing speeds have on the lateral dimensions of graphene. Following literature, the same sample preparation was used with adjustments done to the spin speed and reduced to the lowest rate which our instrument would allow, 300 rpm. This had a positive effect on our thermal conductivity giving a substantial increase from $1 \text{ Wm}^{-1}\text{K}^{-1}$ to $2.24 \text{ Wm}^{-1}\text{K}^{-1}$. Generally, it is speculated that as the mixing rate increases, lateral dimensions of the graphene flakes become smaller which directly affect the overall thermal conductivity of the system.⁴

Having established the effects which a lower mixing speed has on our TIM, we then tried a hybrid style of mixing. The hope in these experiments was to find different forms of agitations to vary the dimension of the graphene flakes and see if by varying the processing this would have a positive effect on our TIMs thermal conductivity. All samples were prepared using mineral oil with 20 wt% of graphene filler. Within these samples 75% of the graphene used was mixed in a slow method, the remaining 25% was mixed at a high speed shear mixed. The goal of varying the parameters was to vary the graphene flake size so that the smaller flakes would fill voids increasing the network of larger flakes and ideally improve the thermal properties.⁵ This method showed enhancement of 100% compared to the samples prepared with all of the filler being mixed at a high speed shear rate of 2500 rpm. The next sample followed similar parameters where 75% of the graphene filler was

mixed at 300 rpm and 25% now was sonicated for 30 minutes, showing again improvement compared to mixing at 2500 rpm but not enough to become an ideal.

The last comparison method was flake size and flake source. All of the samples were prepared using high quality commercially available graphene. For the first experiments the graphene was purchased from graphene supermarket (GS) which the lateral dimensions ranged in size from $\sim 2 \mu\text{m}$ to $\sim 8 \mu\text{m}$ while the thickness varied from single atomic planes of 0.35 nm to ~ 12 nm. The next samples were then purchased from XG Sciences, $\sim 15 \mu\text{m}$ and $\sim 25 \mu\text{m}$ in lateral dimensions respectively.^{4,6} Use of the larger dimensioned graphene flakes saw an improvement of nearly 500% in the thermal conductivity, using a slow mixing method.

Table 3.1: Effect of various preparation parameters on the thermal conductivity of the TIMs with 20 wt% of graphene filler loading kept constant.

Mixing Speed	Graphene Source	Dimensions (μm)	Thermal Conductivity ($\text{Wm}^{-1}\text{K}^{-1}$)
2500 rpm	Graphene Supermarket	2 – 8	1
300 rpm	Graphene Supermarket	2 – 8	2.24
75% at 300 rpm + 25% at 2500 rpm	Graphene Supermarket	2 – 8	2
75% at 300 rpm + 25% sonicated	Graphene Supermarket	2 – 8	2.18
300 rpm	XG Sciences	15	4.92
300 rpm	XG Sciences	25	3.88

3.4 Scanning Electron Microscopy Characterization

SEM is commonly used throughout the scientific community for various imaging needs, where optical microscopy is limited. This technique has a wide array of applications and benefits. The information obtained gives detailed three-dimensional images and

topological details unobtainable using a tradition optical microscope. In this work SEM was used to observe the flake orientation and general flake size post sample preparation. The sample in Figure 3.4 (a-b) is of a high loading fraction sample with 40 wt% graphene filler. The purchased graphene flakes (XG Science) show various orientations within the matrix. The brighter regions are edges of the flakes facing perpendicularly to the plane of the wafer, carrying them. Non-planar orientations are ideal for TIMs because they provide a direct route for thermal transfer to happen within the samples.

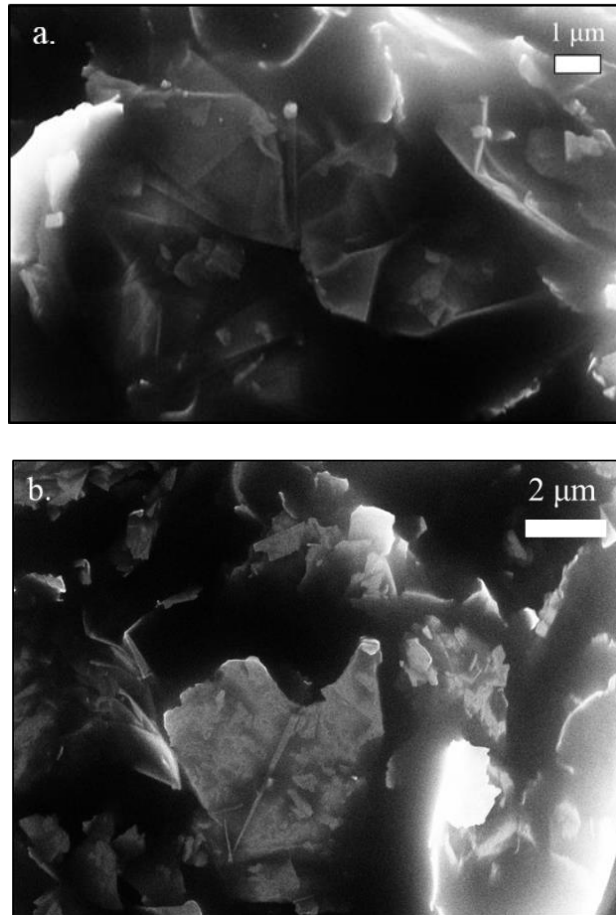


Figure 3.4: SEM images show graphene flakes in noncuring TIM paste.

3.5 Raman Spectroscopy

Raman spectroscopy is a non-destructive measurement technique which measures the inelastic scattering of light within the material. It is widely a used technique in the structural characterization of graphitic materials. Its effect is based on the inelastic scattering of light with atomic lattice of a material resulting in the annihilation or creation of a phonon.⁷ It is an effective technique which helps identify crystallinity, stoichiometry, thickness and defects within a material.⁸ It has been demonstrated as one of the most convenient tools for identifying and counting graphene layers.⁹ Figure 3.5 shows the Raman spectrum of pristine mineral oil (blue curve) and mineral oil with 40 wt% graphene fillers (red curve). The most notable features of the spectrum for graphene are G peak at $\sim 1580\text{ cm}^{-1}$ and 2D peak at $\sim 2700\text{ cm}^{-1}$ G peak originates from the in-plane vibration of the sp^2 carbon atoms and is a double degenerate phonon mode at the center of the Brillouin zone.^{8,9} The intensity of the G peak increases as the number of graphene layer increases. The 2D peak originates from a two phonon double resonance.⁹ The blue curve in Figure 3.5 is the Raman spectra of a 40 wt% fraction of graphene in mineral oil sample verifying the presence of the G, 2D, and D peak, indicating towards few layer graphene.¹⁰ Raman spectroscopy validated the quality of the material post treatment with acetone and high sheer spinning, as well as give an idea as to whether the graphene was chemically changing due to interactions with the mineral oil.

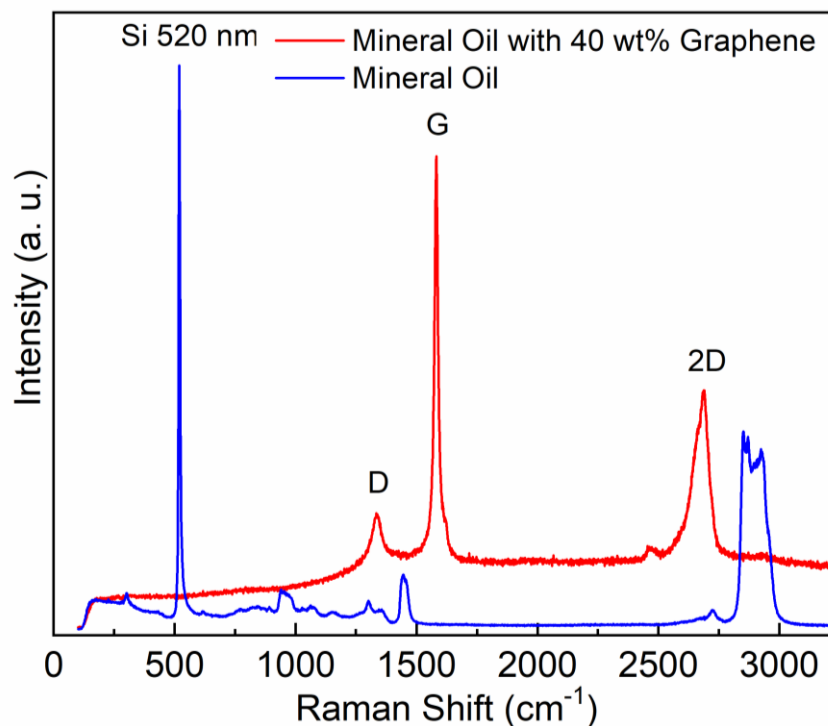


Figure 3.5: Raman spectra of noncuring graphene thermal interface material, with a weight fraction of 40 wt% graphene fillers. Raman was used to verify the homogeneity of the graphene within the TIM post material development.

3.6 Rheological Properties of Non-Graphene TIMs

Rheology is the study of the flow of materials. The instruments used for these experiments is a rheometer and it establishes the viscosity of a material. Viscosity of noncuring thermal interface materials is an important parameter to establish.^{3,11} Easy application is important for industrial needs and mass use of them. Liquids are defined as materials which deform under continuous stress; elastic solids can resist this stress by deformation, where a fluid cannot.¹² Viscoelastic fluids have a mix of properties where they have characteristics of both solids and liquids. Two terms are used frequently with rheometric studies, stress and

strain. Stress is the force per unit area, strain is the amount of deformation over a given distance or length. If the force applied is parallel to the surface, it is called shear stress. A material's resistance to shear stress is its viscosity. Viscosity is measured in centipoise [1 cP = 1 gcm⁻¹s⁻¹].

The relationship between shear stress and shear strain defines properties which give a better understanding to the concept of viscosity, such as Newtonian, pseudoplastic, dilatant and Bingham plastic, shown in Figure 3.6. In Newtonian fluids, the relationship between shear stress and shear rate is linear. These fluids continue to exhibit fluid like behavior even with the increasing amounts of applied shear force and the viscosity is dependent solely on temperature, pressure, and chemical composition. Non-Newtonian fluids have non-linear dependence of shear stress and shear rate and include pseudoplastics and dilatants.

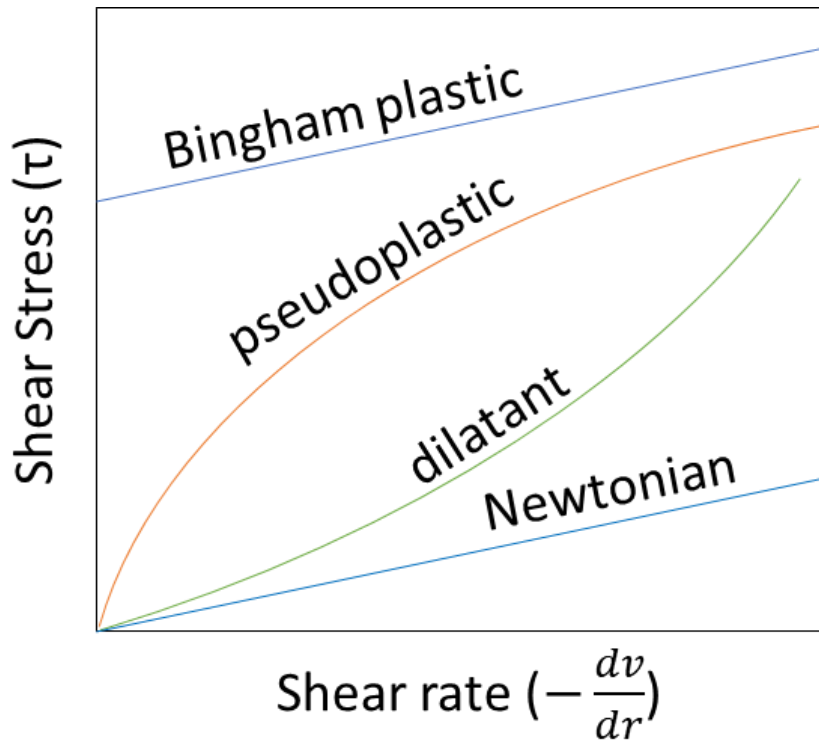


Figure 3.6: Relationship between shear stress and shear rate for various Newtonian and non-Newtonian fluids. The relationship between these two observations is used to define the robustness and longevity of a TIM.

For the study of TIMs, these parameters are important because when developing these composites, pump-out of material is an issue.¹³⁻¹⁵ Pump-out or bleeding out is when the viscosity of the grease changes over various cycles of increased temperature causing the TIM to flow out of the confined interfaces which it is binding. This is a common problem, that is largely due to temperature cycling and the coupling of the filler to the base. We measured these rheological effects of our noncuring graphene based TIM at the weight fraction of 0 wt%, 5 wt% and 10 wt%.

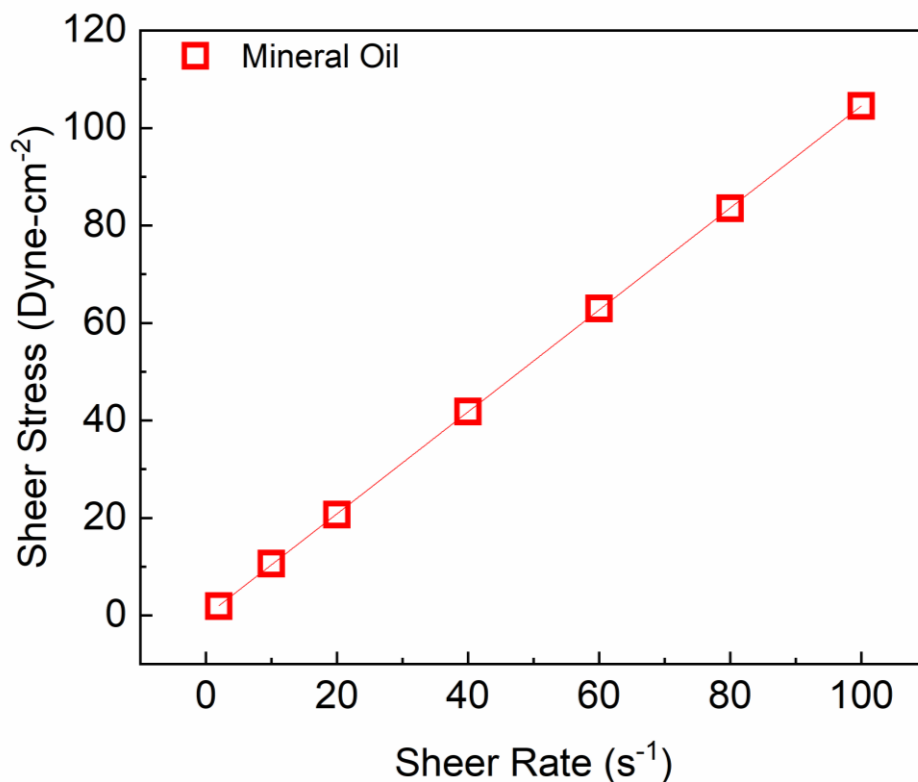


Figure 3.7: Rheological properties of the mineral oil confirming its Newtonian fluid behavior.

The data shown in Figure 3.7 through 3.9 identify the rheometric effects which the graphene fillers have on the mineral oil base. Figure 3.7 is the mineral oil alone and shows Newtonian behavior. Figure 3.7 show the rheological properties of the mineral oil with the addition of graphene fillers at 5 wt% and 10 wt% fractions. Shown in Figure 3.8, TIMs with 5 wt% graphene demonstrates a pseudo plastic behavior. Pseudoplasticity is when a material exhibits both Newtonian flow and plastic flow. The liquid will flow as plastic at high shear rates and the more stress that is applied the more freely it flows.¹⁶⁻¹⁸ The further addition of graphene filler at 10 wt% loading fractions sees a shift into Bingham plastic (Figure 3.9) where the body of the substance is rigid at low stress and flows once an initial

amount of stress is applied, which is the y-intercept here.

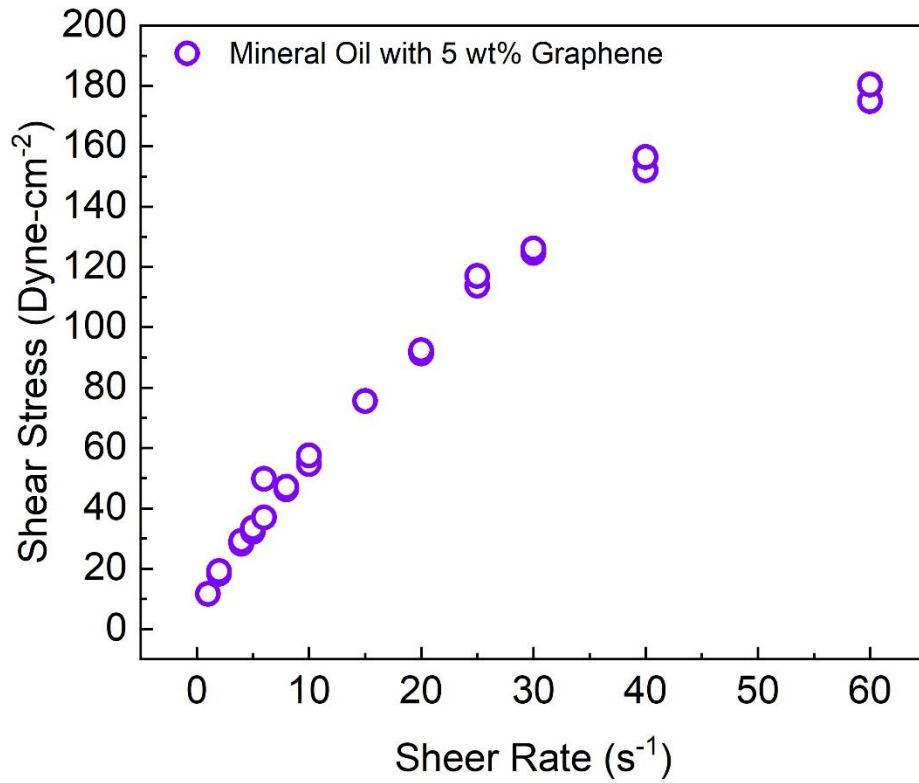


Figure 3.8: Rheological properties of mineral oil with 5 wt% of graphene. The results show a sup-linear behavior of shear stress as a function of shear rate confirming the pseudo plastic properties of the compound.

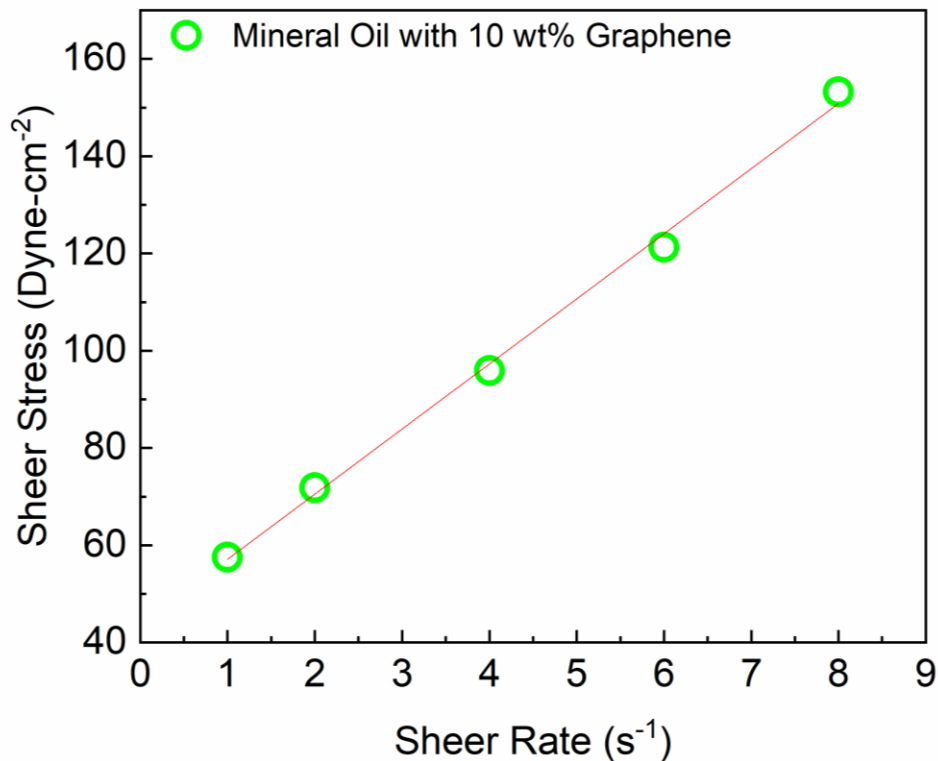


Figure 3.9: Rheological properties of the mineral oil with 10 wt% of graphene loading. The results show a linear behavior of shear stress as a function of shear rate with a positive y-intercept confirming the Bingham plastic behavior of the compound, where an initial stress must be applied for the substance to become liquid.

3.7 Summary and Conclusions

The chapter is an overview of the various techniques used to thoroughly characterize mechanical and thermal properties of TIMs. The determining factor in producing high performing TIMs lies in sample preparation as well as the filler and matrix chosen. Various experiments were performed to find the ideal parameters for sample preparation and a method of slowly mixing our graphene flakes with mineral oil and acetone gave the highest thermal conductivity. The high thermal conductivity value achieved is attributed to reduced

agitation of our flakes while mixing, which allows them to retain their dimensions in our final TIM. Raman spectroscopy was used to determine the composition of the TIM and evaluate whether any degradation or reduction of graphene occurred. A steady state method (TIM tester) was used in the evaluation of the thermal properties of our TIM and help determine our process parameters as well as gave the flexibility in allowing for other experimental setups discussed in later chapters, such as pressure dependence as well as temperature dependence measurements. SEM is a widely used technique which was used to characterize the flake dimensions in the 40 wt% graphene filler in mineral oil TIM. Lastly, a rheometer was used to determine the fluidity and viscosity of our TIM, this technique showed transition with the addition of small wt% of graphene, transition from Newtonian with pure mineral oil to a Bingham plastic with 10 wt% of graphene in mineral oil. Proper evaluation and preparation of TIM is important to the integrity of the material created and can be a way to properly take advantage of a materials inherent thermal conductivity in a composite.

References

1. D4570-17, A. *Standard Test Method for Thermal Transmission Properties of Thermally Conductive Electrical Insulation Materials 1*. (ASTM International, 2017). doi:10.1520/D5470-17
2. Tian, X., Itkis, M. E., Bekyarova, E. B. & Haddon, R. C. Anisotropic Thermal and Electrical Properties of Thin Thermal Interface Layers of Graphite Nanoplatelet-Based Composites. *Scientific Reports* **3**, 1710 (2013).
3. Mehrali, M., Sadeghinezhad, E., Latibari, S. T., Kazi, S. N., Mehrali, M., Zubir, M. N. B. M. & Metselaar, H. S. C. Investigation of Thermal Conductivity and Rheological Properties of Nanofluids Containing Graphene Nanoplatelets. *Nanoscale Research Letters* **9**, 15 (2014).
4. Xu, X., Pereira, L. F. C., Wang, Y., Wu, J., Zhang, K., Zhao, X., Bae, S., Tinh Bui, C., Xie, R., Thong, J. T. L., Hong, B. H., Loh, K. P., Donadio, D., Li, B. & Özyilmaz, B. Length-Dependent Thermal Conductivity in Suspended Single-Layer Graphene. *Nature Communications* **5**, 3689 (2014).
5. Shahil, K. M. F. & Balandin, A. A. Thermal Properties of Graphene and Multilayer Graphene: Applications in Thermal Interface Materials. *Solid State Communications* **152**, 1331–1340 (2012).
6. Goyal, V. & Balandin, A. A. Thermal Properties of the Hybrid Graphene-Metal Nano-Micro-Composites: Applications in Thermal Interface Materials. *Applied Physics Letters* **100**, 073113 (2012).
7. Fugallo, G., Cepellotti, A., Paulatto, L., Lazzeri, M., Marzari, N. & Mauri, F. Thermal Conductivity of Graphene and Graphite: Collective Excitations and Mean Free Paths. *Nano Letters* **14**, 6109–6114 (2014).
8. Calizo, I., Balandin, A. A., Bao, W., Miao, F. & Lau, C. N. Temperature Dependence of the Raman Spectra of Graphene and Graphene Multilayers. *Nano Letters* **7**, 2645–2649 (2007).
9. Ferrari, A. C., Meyer, J. C., Scardaci, V., Casiraghi, C., Lazzeri, M., Mauri, F., Piscanec, S., Jiang, D., Novoselov, K. S., Roth, S. & Geim, A. K. Raman Spectrum of Graphene and Graphene Layers. *Physical Review Letters* **97**, 187401 (2006).
10. Nika, D. L., Ghosh, S., Pokatilov, E. P. & Balandin, A. A. Lattice Thermal Conductivity of Graphene Flakes: Comparison with Bulk Graphite. *Applied Physics Letters* **94**, 203103 (2009).
11. Kole, M. & Dey, T. K. Investigation of Thermal Conductivity, Viscosity, and

- Electrical Conductivity of Graphene Based Nanofluids. *Journal of Applied Physics* **113**, 084307 (2013).
12. Macosko, C. W. & Larson, R. G. *Rheology: Principles, Measurements, and Applications*. (Wiley-VCH Verlag, 1994).
 13. Gwinn, J. P. & Webb, R. L. Performance and Testing of Thermal Interface Materials. in *Microelectronics Journal* **34**, 215–222 (2003).
 14. Hansson, J., Zandén, C., Ye, L. & Liu, J. Review of Current Progress of Thermal Interface Materials for Electronics Thermal Management Applications. in *16th International Conference on Nanotechnology - IEEE NANO 2016* 371–374 (2016). doi:10.1109/NANO.2016.7751383
 15. Otiaba, K. C., Ekere, N. N., Bhatti, R. S., Mallik, S., Alam, M. O. & Amalu, E. H. Thermal Interface Materials for Automotive Electronic Control Unit: Trends, Technology and R&D Challenges. *Microelectronics Reliability* **51**, 2031–2043 (2011).
 16. Scriven, L. E. Dynamics of a Fluid Interface Equation of Motion for Newtonian Surface Fluids. *Chemical Engineering Science* **12**, 98–108 (1960).
 17. Prasher, R. Thermal Interface Materials: Historical Perspective, Status, and Future Directions. *Proceedings of the IEEE* **94**, 1571–1586 (2006).
 18. Sarmiento, G., Crabbe, P. G., Boger, D. V. & Uhiherr, P. H. T. Measurement of the Rheological Characteristics of Slowly Settling Flocculated Suspensions. *Industrial and Engineering Chemistry Process Design and Development* **18**, 746–751 (1979).

Chapter 4: Noncuring Graphene Thermal Interface Materials for Advanced Electronics

4.1 Introduction

As transistors continue to decrease in size and packing densities increase, thermal management becomes the critical bottleneck for development of next generation of compact and flexible electronics.¹ The increase in computer usage and ever-growing dependence on cloud systems require better methods for dissipating heat away from electronic components. The important ingredients of thermal management are TIMs. Various TIMs interface two uneven solid surfaces where air would be a poor conductor of heat, and aid in heat transfer from one medium into another. Two important classes of TIMs include curing and noncuring composites. Both of them consist of a base, *i.e.* matrix materials, and thermally conducting fillers. Commonly, the studies of new fillers for the use in TIMs start with the curing epoxy-based composites owing to the relative ease of preparation and possibility of comparison with a wide range of other epoxy composites. Recent work on TIMs with carbon fillers have focused on curing composites, which dry to solid.²⁻⁷ Curing TIMs are required for many applications, *e.g.* attachment of microwave devices, but do not cover all thermal management needs. Thermal management of computers requires specifically noncuring TIMs, which are commonly referred to as thermal pastes or thermal greases. They are soft pliable materials, which unlike cured epoxy-based composites, or phase change materials, remain soft once applied. This aids in avoiding crack formations in the bond line due to repeated thermal cycling of two

connected materials with different temperature expansion coefficients. Noncuring TIMs also allow for easy reapplication, known as a TIM's re-workability property. Noncuring TIMs are typically cost efficient – an essential requirement for commercial applications. Various applications in electronics, noncuring grease-like (soft) TIMs are preferred. Examples of the applications include but are not limited to cooling of large data centers⁸ and personal devices which are the primary targets for these applications. Current commercially available TIMs perform in thermal conductivity range of $0.5 \text{ Wm}^{-1}\text{K}^{-1}$ to $5 \text{ Wm}^{-1}\text{K}^{-1}$ with combination of several fillers at high loading fractions⁹. State-of-the-art and next generation electronic devices require thermal pastes with bulk thermal conductivity in the range of 20 to $25 \text{ Wm}^{-1}\text{K}^{-1}$.^{10,11} This study focuses specifically on noncuring TIMs with graphene and few-layer graphene fillers.

Curing and noncuring TIMs consists of two main components – a polymer or oil material as its base and fillers, which are thermally conductive inclusions added to the base increasing the overall heat conduction properties of the resulting composite. Polymer base materials have a rather low thermal conductivity within the range of $0.2 \text{ Wm}^{-1}\text{K}^{-1}$ to $0.5 \text{ Wm}^{-1}\text{K}^{-1}$, mainly owing to their amorphous structure.¹² The strategy for creating advanced TIM is to find a filler with high intrinsic thermal conductivity and incorporate it into a base creating a soft material, which is easy to apply and bind the interfaces. Numerous other parameters such as filler – matrix coupling, uniformity of the dispersion of the fillers, viscosity, and surface adhesion affect the resulting performance of the TIM. Conventional fillers, which are added to enhance the thermal properties of the base polymeric or oil matrices, span a wide range of materials, including metals,^{13,14} ceramics, metal oxides,^{15–}

²⁰ and semiconductors^{18,21} with micro and nanometer scale dimensions. Apart from thermal conductivity, the selection criteria for fillers include many parameters such as compatibility with the matrix, weight, thermal expansion characteristics and rheological behavior. Recent concerns over environmentally friendly materials further limit the list of available additives, which can be used as fillers. Considering all these parameters and limitations, the most promising recently emerged filler material is graphene.^{22,23}

The first exfoliation of graphene^{24,25} and measurement of its electrical properties sparked intensive efforts to find graphene's applications in electronics,²⁶ *e.g.* as on-chip or inter-chip²⁷ interconnects,^{28,29} or a complementary material to silicon in analog or non-Boolean electronics.³⁰ The idea of using graphene as fillers in thermal applications emerged from the discovery of the exceptional heat conduction properties of suspended “large” flakes of single layer graphene (SLG), with the thermal conductivity ranging from 2000 $\text{Wm}^{-1}\text{K}^{-1}$ to 5300 $\text{Wm}^{-1}\text{K}^{-1}$.^{31,32} It is established that acoustic phonons are the main heat carriers with the “gray” mean-free-path (MFP) of ~ 750 nm. Theory suggests that long-wavelength phonons with much larger MFP make substantial contribution to thermal conductivity. The thermal conductivity of SLG with lateral dimensions smaller than MFP degrades due to the “classical size” effects, *i.e.* phonon – flake edges scattering. The thermal conductivity of SLG is vulnerable to defects, wrinkles, bending, and rolling.³³ The cross-section of SLG is also small making it not an ideal filler. From another perspective, FLG is more resistant to degradation of its intrinsic thermal properties due to rolling, bending or exposure to matrix defects. For these reasons, FLG with some addition of SLG, create better filler-matrix and filler-filler coupling, and are considered to be optimum filler

mixture. The in-plane thermal conductivity of FLG converges to that of the high quality bulk graphite, which by itself is as high as $\sim 2000 \text{ Wm}^{-1}\text{K}^{-1}$, as the number of layers exceeds about eight mono-layers.^{34–36} The ability of FLG – a van der Waals material – to present thermal conductivity of bulk graphite is an important factor for thermal applications. The thermal conductivity of FLG is one and two orders of magnitudes higher than that of the conventional metallic and ceramics fillers, respectively.

Technological challenges using graphene and FLG as fillers in thermal management applications, which by their nature requires large amount of source material, were linked to the low yield production laboratory methods. The last decade of graphene research has led to development of several scalable techniques, such as liquid phase exfoliation (LPE)^{37,38} and graphene oxide reduction,^{39,40} which provide large quantities of graphene and FLG of quality acceptable for thermal applications, making the mass production cost effective.^{38,41} These recent developments remove the barriers for graphene utilization in the next generation of curing and noncuring TIMs. In the following discussion, in thermal context, we will use the term “graphene” for the mixture of mostly FLG with some fraction of SLG. When required the term FLG will be used to emphasize its specific thickness. One should note that, in the considered thickness range, FLG retains its flexibility and remains different from brittle thin films of graphite.

To date, the studies of graphene fillers in TIMs were focused almost exclusively on curing epoxy-based composites. The pioneering studies reported the thermal conductivity enhancement of epoxy by a factor of $25\times$ even at small graphene loading fractions of $f_g = 10 \text{ vol}\%$.^{42,43} The only available reports of graphene enhanced noncuring TIMs utilized

commercial TIMs with addition of some fraction of graphene fillers. It has been shown that incorporation of small loading fraction graphene fillers into commercial noncuring TIMs enhances their thermal conductivity significantly.^{42,44-47} However, in view of undisclosed composition of commercial TIMs it is hard to assess the strength of the effect of graphene fillers. In addition, commercial TIMs already have a high concentrations of fillers, and the addition of even a small amount of graphene results in agglomeration and creation of separated clusters of fillers. These facts motivated the present research, which uses the simple base such as mineral oil and in-house process of preparation and incorporation of graphene fillers.

Combining different types of fillers with various sizes and aspect ratios into a single matrix for achieving the “synergistic effects” is a known strategy for attaining a further enhancement in thermal properties of composites.^{11,17} It has been demonstrated that the “synergistic effects” are effective even when one uses fillers of the same material but with two or more size scales.^{6,17} A simple explanation for this effect is that smaller size fillers reside between large fillers and connected them more efficiently, leading to improved thermal conduction. By their nature, FLG fillers consist of several graphene monolayers which are held up through weak Van der Waals forces⁴⁸ in the cross-plane direction. During the mixing processes of FLG with the matrix materials, due to the high shear stresses involved, the atomic layers of FLG separate out, resulting in a mixture of FLG and SLG fillers, which potentially develop reveal the “synergistic effect”. The FLG fillers are better for heat conduction while SLG fillers are more flexible and better for establishing the links

among the FLG fillers. These properties can be considered extra advantages of FLG over metallic and ceramic fillers.

4.2 Material Synthesis and Characterization

Figure 4.1 illustrates the step-by-step preparation procedure and typical applications of noncuring TIMs in electronics. Commercially available graphene fillers (grade H-15, XG-Sciences) with the vendor-specified large lateral dimensions of $\sim 15 \mu\text{m}$ were weighed and added in pre-calculated proportions to the mineral oil base (Walgreen Health). The large lateral dimensions of the fillers are essential for achieving high thermal conductivity. However, it should be noted that large fillers are more susceptible to rolling and bending during the mixing procedure³ so special care should be taken in order to avoid filler agglomeration and crumbling, especially at high filler loading fractions. In order to avoid agglomeration, the mixtures of mineral oil and graphene were prepared with addition of acetone in order to keep the filler quality and size intact during the mixing process.⁴⁹⁻⁵¹ Adding a solvent such as acetone to the fillers lowers the impact, which mixing has on the fillers as well as on the dispersion of the TIM.^{37,52,53} Graphene is measured and placed into a container followed by the addition of acetone, creating a graphene-acetone suspension, then the mineral oil is added. The compounds are mixed using a high shear speed mixer (Flacktek Inc.) at 310 rpm, the lowest mixing speed, for about 20 minutes. The effects of mixing speed and other parameters have been researched in details and utilized in the preparation.^{51,54} The hydrophobicity of graphene explains the mechanism of creation of the emulsion, and the graphene's preference in binding to the oil over acetone.⁵⁵ The low mixing speed results in the binding of graphene and mineral oil, and separates them from

the acetone which has been added later. The acetone is removed from graphene and mineral oil mixture following phase separation. Finally, the mixture is placed in an oven to evaporate the solvent for ~2 hours at 70° C. This process yields a smooth paste with proper viscosity that is easily spreadable, homogenous, and can be contained within a syringe for later applications. The prepared samples have been characterized using Raman spectroscopy and SEM (Figure 3.5 & Figure 3.6). The homogenous dispersion of graphene inside the paste is important to the integrity of the composite.⁵⁶ In addition to good filler dispersion, a preservation of the fillers throughout the process is another important factor in the performance of the obtained noncuring TIMs.

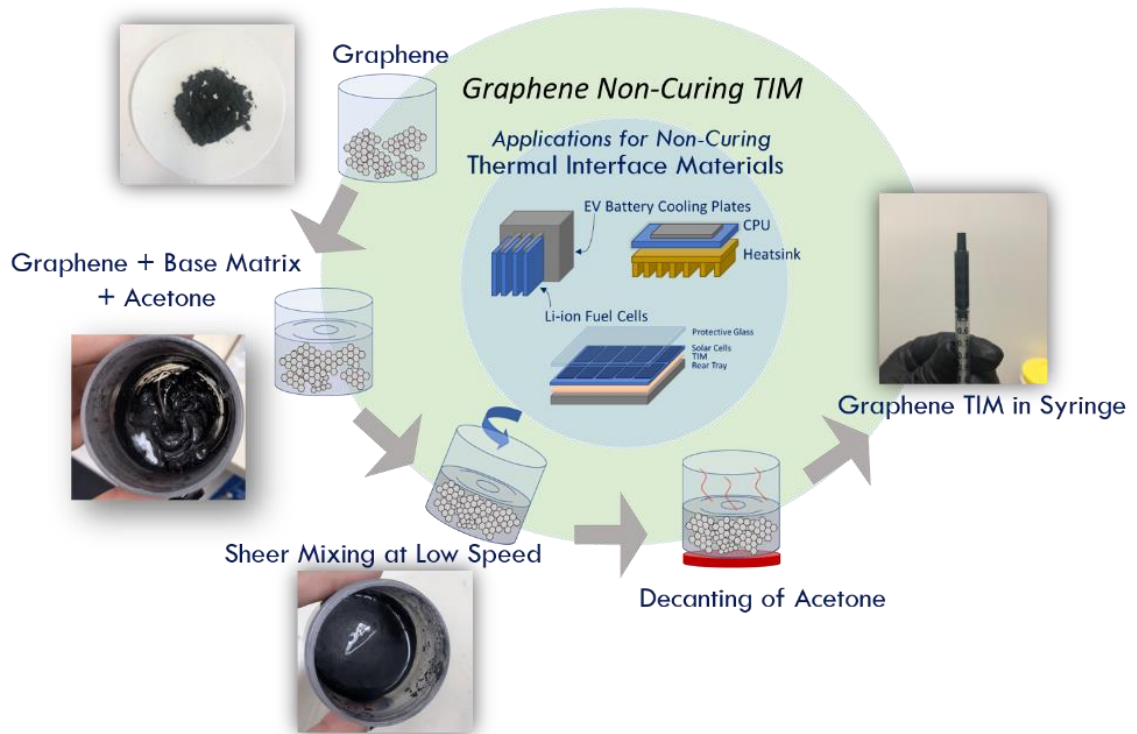


Figure 4.1: Schematic showing typical practical applications of noncuring thermal interface materials in electronics, and the process flow for synthesizing graphene noncuring thermal paste. Graphene is added to the base material with acetone followed by the slow speed shear mixing. The optimized mixing process separates the graphene and mineral oil mix from the acetone. This leaves a smooth graphene paste with proper viscosity which is easy to store and apply at the interfaces. Reprinted with permission from Advanced Electronic Materials. The data is from Naghibi, S., Kargar, F., Wright, D., Huang, C. Y. T., Mohammadzadeh, A., Barani, Z., Salgado, R. & Balandin, A. A. Noncuring Graphene Thermal Interface Materials for Advanced Electronics. *Advanced Electronic Materials* 1901303 (2020). doi:10.1002/aelm.201901303.

The thermal conductivity and contact resistance of the samples were measured using an industrial grade TIM tester (LonGwin Science and Technology Corp.) designed for measurements according to the standard ASTM D 5470-06 – a steady-state method for measuring the thermal properties of TIMs.⁵³ This method is based on the one-dimensional heat conduction Fourier’s law, $q'' = -k_{app}\Delta T/\Delta x$, which allows for determining the sample’s *apparent* thermal conductivity, k_{app} [$\text{Wm}^{-1}\text{K}^{-1}$], *via* accurately monitored heat

conduction flux, q'' [Wm^{-2}], and the temperature difference, ΔT [K], across the sample's thickness, Δx [m^{-1}]. The sample's total thermal resistance per area, $R''_{tot} = \Delta T/q'' = \frac{\Delta x}{k_{app}}$ [Km^2W^{-1}], at various thicknesses were measured at a constant temperature of 35 °C, atmospheric pressure, and plotted as a function of its thickness. The data has been fitted using a linear regression method. The inverse slope and the y-intercept of the fitted line shows the TIM's thermal conductivity and twice of its thermal contact resistance, $2R''_c$,⁵⁷ as explained below in more details. The temperature dependent thermal conductivity measurements are conducted in the same way, only changing the temperature in the range of 30 °C to 115 °C, with no applied pressure.

4.3 Results of Thermal Testing

When a thin layer of TIM is applied between two solid surfaces, assuming a one-dimensional heat flow from the hot to the cold side, the total thermal resistance can be defined as $R''_{tot} = R''_{TIM} + R''_{c1} + R''_{c2}$ where R''_{TIM} is the thermal resistance associated with the TIM layer and R''_{c1} and R''_{c2} are the thermal contact resistances between the TIM and solid surfaces due to the inherent microscopic asperities within solid surfaces. This equation can be restated as $R''_{tot} = BLT/k_{app} = BLT/k_{TIM} + 2R''_c$ considering that the thermal contact resistance between the TIM layer and upper and lower solid surfaces are equal ($R''_{c1} = R''_{c2} = R''_c$). In this equation, k_{app} and k_{TIM} are the *apparent* and the “bulk” thermal conductivity of the TIM layer. The difference between these two quantities is that the former depends on bond line thickness (BLT) and the thermal contact resistances and thus, is not a material property, which is why it is referred as “apparent” thermal conductivity. However, the latter is related to the “true” or “bulk” thermal conductivity of the TIM layer which is a material

characteristic and depends on the thermal transport properties of the base polymeric matrix, fillers, and their interaction with each other.

In Figure 4.3, we show the results of R''_{tot} measurements of TIMs with different filler loadings as a function of the BLT at a constant temperature of 35 °C without any applied pressure (atmospheric pressure). Since R''_{tot} depends linearly on BLT, one can extract k_{TIM} and R''_c with linear fittings (dashed lines in Figure 4.2) on the experimental data. In this case, the inverse slope and the y-intercept of the fitted line shows k_{TIM} and $2R''_c$, respectively, with an assumption that both parameters remain constant as BLT changes. As one can see, with adding graphene fillers, the slope of the fitted lines decreases significantly, indicating a strong enhancement in the “bulk” thermal conductivity of the compound. However, addition of fillers also increases the thermal contact resistance, which will be discussed later.

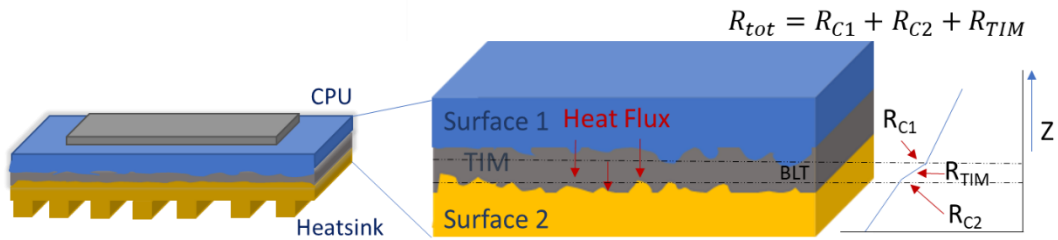


Figure 4.2: The above schematic highlights the resistance which two uneven surfaces creates with respect to the TIM and the direction of the heat flux. Reprinted with permission from Advanced Electronic Materials. The data is from Naghibi, S., Kargar, F., Wright, D., Huang, C. Y. T., Mohammadzadeh, A., Barani, Z., Salgado, R. & Balandin, A. A. Noncuring Graphene Thermal Interface Materials for Advanced Electronics. *Advanced Electronic Materials* 1901303 (2020). doi:10.1002/aelm.201901303.

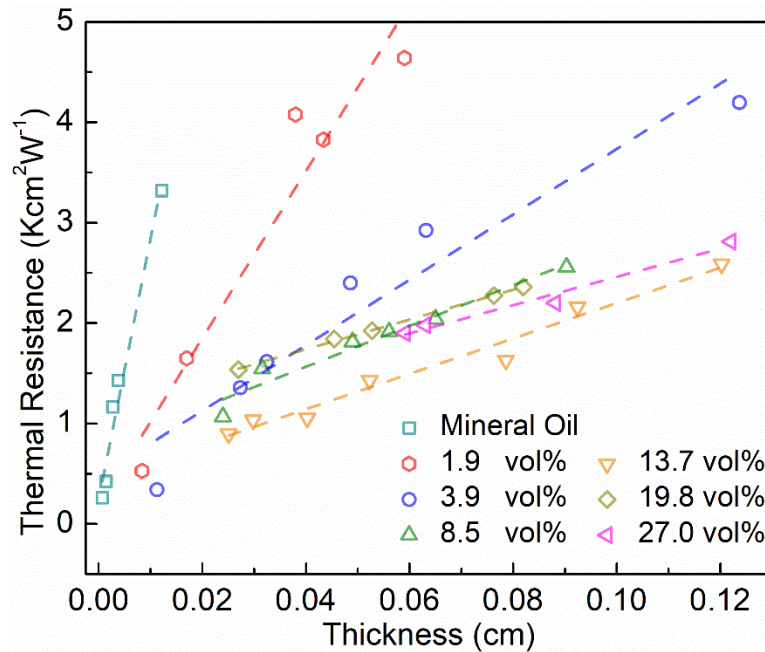


Figure 4.3: Thermal resistance per unit area, R'' , as a function of the bond line thickness. The dashed lines show the linear regression fittings to the experimental data. Adding graphene fillers to mineral oil results in the slope of the lines decreasing significantly, indicating string enhancement in the “bulk” thermal conductivity of the graphene thermal paste. Reprinted with permission from Advanced Electronic Materials. The data is from Naghibi, S., Kargar, F., Wright, D., Huang, C. Y. T., Mohammadzadeh, A., Barani, Z., Salgado, R. & Balandin, A. A. Noncuring Graphene Thermal Interface Materials for Advanced Electronics. *Advanced Electronic Materials* 1901303 (2020). doi:10.1002/aelm.201901303.

Figure 4.4 presents the thermal conductivity of the graphene noncuring TIMs as a function of the filler loading. The error bars are associated with the standard error in the thermal conductivity measurements as a result of the linear fitting through the experimental data shown in Figure 4.3. The data indicates that at small, $\phi = 1.9$ vol%, graphene filler loading, a significant enhancement in compound’s thermal conductivity is observed followed by a saturation effect at the higher loading fractions. This enhancement is attributed to the thermal percolation, i.e. the onset of formation of the continuous network of thermally conductive fillers inside the matrix. The thermal percolation strongly enhances

the overall thermal conductivity of the composites. Note that the thermal conductivity increases from $0.3 \text{ Wm}^{-1}\text{K}^{-1}$ of pure mineral oil to $1.2 \text{ Wm}^{-1}\text{K}^{-1}$ with addition of only 1.9 vol% of graphene. The observed change in the thermal conductivity is similar to the electrical conductivity behavior of polymers as they are loaded with electrically conductive fillers.⁵⁸

In the electrical percolation regime, the electrical conductivity of polymers increases by several orders of magnitude as electrically conductive fillers form a continuous network inside the electrically insulating matrix. The electrical percolation is theoretically described by the power scaling law as $\sigma \sim (\phi - \phi_E)^t$, where σ is the electrical conductivity of the composite, ϕ is the filler loading fraction, ϕ_E is the filler loading at the electrical percolation threshold, and t is the “universal” critical exponent. Following the same theoretical concept, the experimental data in Figure 4.4 has been fitted by a power scaling law as $k_{TIM} = A(\phi - \phi_{th})^p$, where k_f is the thermal conductivity of the filler, and A , ϕ_{th} and p are fitting parameters being the filler loading at thermal percolation threshold and the exponent, respectively. The inset in Figure 4.3 shows the experimental data and theoretical fitting in a log-log scale. Generally, as the loading fraction of filler increases, one would expect to see substantial continuous increases in enhancement of TIM’s thermal conductivity. Most cured, *i.e.* solid, TIMs exhibit linear to super-linear thermal conductivity dependence on the filler loading fraction². However, the prepared *noncuring* TIMs exhibit a saturation effect for the thermal conductivity as a function of the filler loading fraction. This is similar to the effect reported previously for nano-fluids and some soft TIMs.^{59–62} The saturation effect is attributed to a tradeoff between the enhancement in

the “bulk” thermal conductivity as more fillers are added to the matrix and the decrease in the thermal conductance as the thermal interface resistance between the filler – filler and filler – matrix interfaces increases due to incorporation of more fillers into the matrix. Note that heat transport in graphene based compounds are dominated by phonons although they reveal electrical percolation at rather low graphene loadingsmmor.^{3,35,63}

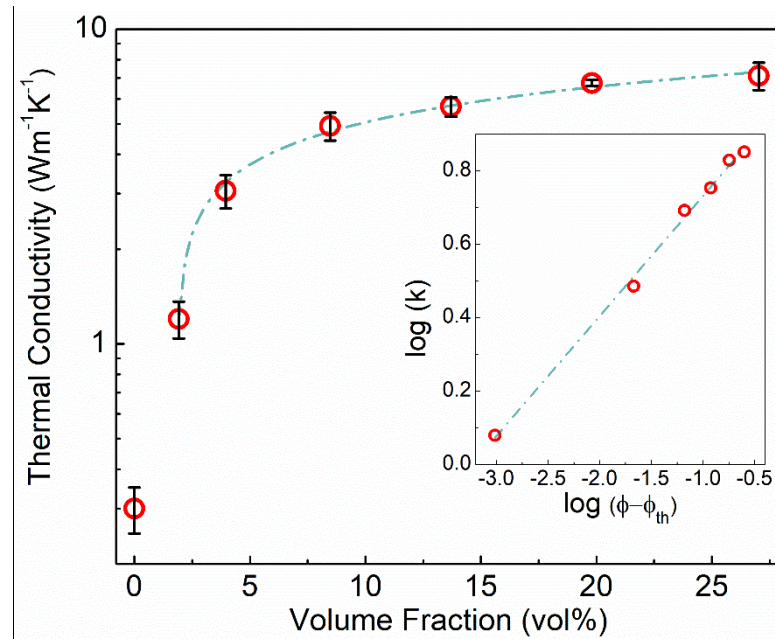


Figure 4.4: Thermal conductivity of the noncuring graphene TIMs as a function of graphene volume fraction. Adding fillers to the mineral oil base leads to more than 4× enhancement of the thermal conductivity at $\phi = 1.9$ vol%. The strong enhancement is attributed to the onset of the thermal percolation. The increase in thermal conductivity slows down as more fillers are incorporated into the matrix, and it saturates at the high loading fractions. The dashed lines are the theoretical fitting of the experimental data according to the effective thermal conductivity equation $k \sim (\phi - \phi_{th})^p$ with $\phi_{th} = 1.9$ vol% and $p = 0.32$. The inset shows the data in a log-log scale. Reprinted with permission from Advanced Electronic Materials. The data is from Naghibi, S., Kargar, F., Wright, D., Huang, C. Y. T., Mohammadzadeh, A., Barani, Z., Salgado, R. & Balandin, A. A. Noncuring Graphene Thermal Interface Materials for Advanced Electronics. *Advanced Electronic Materials* 1901303 (2020). doi:10.1002/aelm.201901303.

Figure 4.5 shows the contact resistance, R_c'' , of the noncuring graphene TIMs as a function of the filler loading fraction measured at the atmospheric pressure. As expected, with incorporation of more fillers into the matrix, the contact resistance increases as well. For semi-solid or semi-liquid TIMs, assuming that the “bulk” thermal conductivity of the TIM layer is much smaller than that of the binding surfaces, the contact resistance can be described using the semi-empirical model as $R_{c_1+c_2}'' = 2R_c'' = c \left(\frac{\zeta}{k_{TIM}} \right) \left(\frac{G}{P} \right)^n$,⁶² where $G = \sqrt{G'^2 + G''^2}$. In this equation, G' and G'' are the storage and loss shear modulus of the TIM, P is the applied pressure, ζ is the average roughness of the two binding surfaces, assuming that both have the same roughness at interfaces, and c and n are empirical coefficients, respectively. One can see that at a constant applied pressure the prediction of thermal contact resistance becomes cumbersome owing to the fact that the two parameters have opposing effects on the contact resistance. The latter is due to the fact that adding graphene fillers results in increasing both k_{TIM} and G . However, this equation intuitively suggests that for TIMs with a specific filler, there exists an optimum filler loading at which the “bulk” thermal conductivity, k_{TIM} , significantly increases while the thermal contact resistance, R_c'' , is affected only slightly. This fact becomes more evident if we restate the total thermal resistance as $R_{tot}'' = \left(\frac{1}{k_{TIM}} \right) \left\{ BLT + c\zeta \left(\frac{G}{P} \right)^n \right\}$ showing the importance of increasing the TIM bulk thermal conductivity to reduce the total thermal resistance.

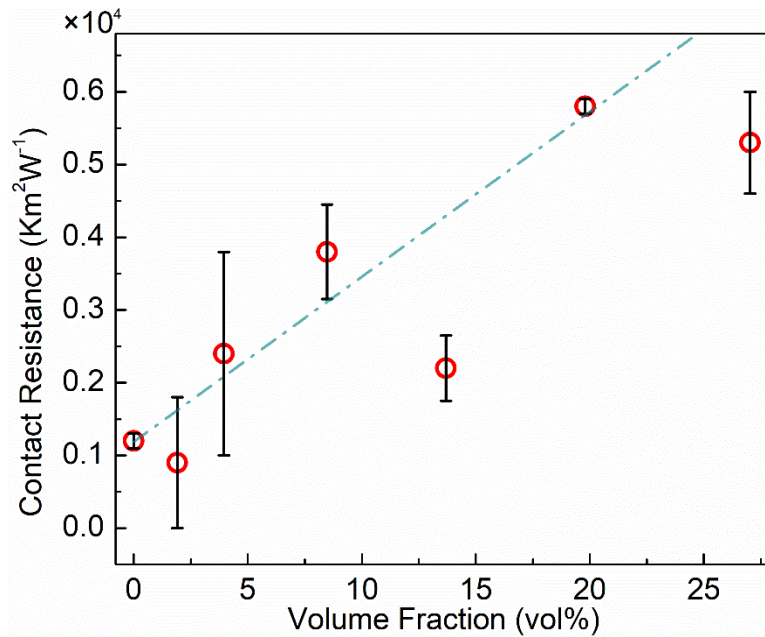


Figure 4.5: Thermal contact resistance as a function of the filler loading. The error bars show the standard error. The thermal contact resistance increases with the loading fraction. Reprinted with permission from Advanced Electronic Materials. The data is from Naghibi, S., Kargar, F., Wright, D., Huang, C. Y. T., Mohammadzadeh, A., Barani, Z., Salgado, R. & Balandin, A. A. Noncuring Graphene Thermal Interface Materials for Advanced Electronics. *Advanced Electronic Materials* 1901303 (2020). doi:10.1002/aelm.201901303.

The temperature of electronic devices during operation, no matter how the generated heat is dissipated, increases due to Joule heating, which is unavoidable. The temperature rise depends on the total thermal resistance of the system from the heat source to the environment. In most cases, the TIM layer is one of the bottlenecks for efficient thermal management of the system. In this process, the temperature across the TIM layer increases which in turn, affects its “bulk” thermal conductivity and thermal contact resistance. In order to evaluate the overall thermal performance of the TIM layer in an extended temperature range, the “apparent” thermal conductivity is a more informative parameter. It includes the temperature effects on both the “bulk” thermal conductivity and

thermal contact resistance. It is important to evaluate the temperature dependent characteristics of noncuring graphene TIMs in order to verify their overall robustness and stability at elevated temperatures. Practically useful TIMs should perform at high temperatures and retain their thermal properties, as well as sustain an uneven heating throughout the component.

In Figure 4.6 we present the “apparent” thermal conductivity of the noncuring graphene TIMs as a function of temperature in the range of 40 °C – 115 °C, with no applied pressure. The data are shown for TIMs with various graphene loading fractions. The noncuring graphene TIMs with $\phi = 1.9$ vol% exhibit a slight variation in the “apparent” thermal conductivity as the temperature increases. The “apparent” thermal conductivity change is more pronounced in TIMs with the higher loading compared to that of TIMs with the low graphene loading, although the change is not significant. Generally, the shear modulus of TIMs decreases with increasing the joint temperature, which, in turn, reduces the thermal contact resistance. However, the “bulk” thermal conductivity of TIMs is also decreasing with temperature,⁶⁴ which causes the overall “apparent” thermal conductivity to drop. At the same time, the decrease in the “apparent” thermal conductivity is not significant, attesting to the practicality of noncuring graphene thermal paste.^{65,66}

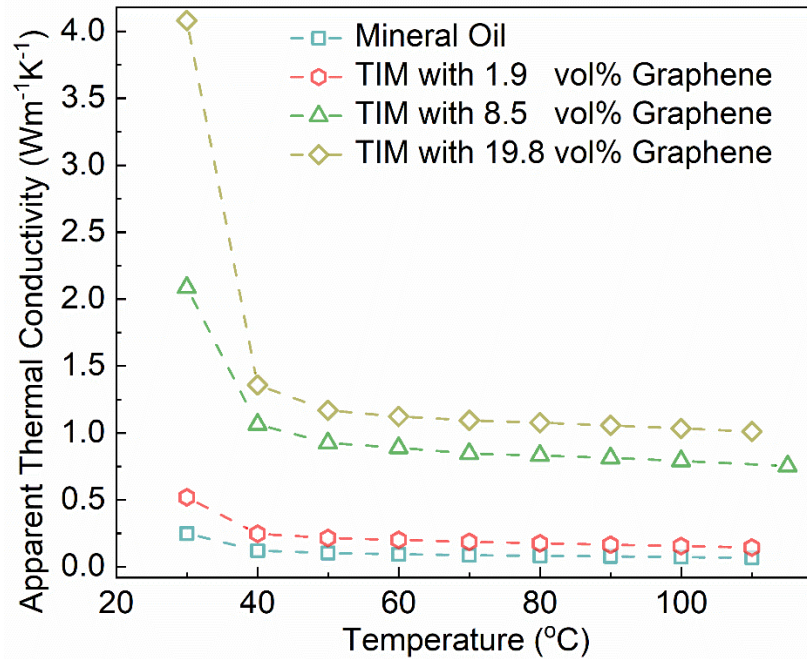


Figure 4.6: “Apparent” thermal conductivity of the non-cured graphene TIMs as a function of temperature in the range from 40 °C to 115 °C. Reprinted with permission from Advanced Electronic Materials. The data is from Naghibi, S., Kargar, F., Wright, D., Huang, C. Y. T., Mohammadzadeh, A., Barani, Z., Salgado, R. & Balandin, A. A. Noncuring Graphene Thermal Interface Materials for Advanced Electronics. *Advanced Electronic Materials* 1901303 (2020). doi:10.1002/aelm.201901303.

Another important issue that arises at increased temperature for non-cured TIMs is “pumping out”, also referred to as “bleeding out” problem.^{9,67,68} This term indicates the process of thermal grease pumping out from the binding surfaces due to the decrease of the viscosity at elevated temperature and continuous temperature cycling of the electronic devices at on-off operational states.⁶⁹ The latter results in reduction of the actual contact of the TIM layer with adjoining solid surfaces, which increases the thermal contact resistance. In order to evaluate the “bleeding out” problem associated with the non-cured graphene TIMs, the BLT variation has been measured as a function of temperature (see Figure 4.7). The variation in BLT as a function of temperature in pure mineral oil and TIM with $\phi =$

1.9 vol% is $\sim 2 \mu\text{m}/^\circ\text{C}$ whereas for the TIM with $\phi = 8.5 \text{ vol}\%$ it drops to $\sim 0.5 \mu\text{m}/^\circ\text{C}$. As one can see, the variation is more pronounced at low graphene loadings as compared to that with the high loading. This observation indirectly indicates that noncuring graphene TIMs with graphene loading of more than $\sim 8.5 \text{ vol}\%$ are less prone to the “bleeding out” problem. More extensive power cycling experiments are needed to determine the application efficiency, stability, and reliability of the produced graphene based noncuring TIMs. These measurements are beyond the scope of the present investigation and reserved for future studies.^{70–72}

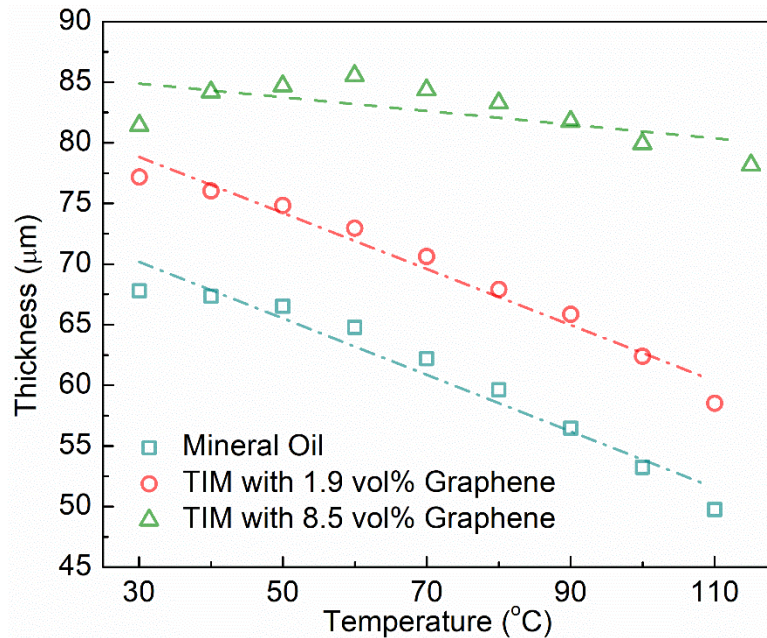


Figure 4.7: Bond line thickness as a function of temperature at atmospheric pressure. The variation in BLT for mineral oil and noncuring graphene TIM with $\phi = 1.9 \text{ vol}\%$ is $\sim 2.3 \mu\text{m}/^\circ\text{C}$. The variation in the TIM thickness with temperature drops to $\sim 0.5 \mu\text{m}/^\circ\text{C}$ at the higher graphene filler loading. The latter indicates the noncuring graphene TIMs with higher graphene loading are less prone to the “bleeding-out” problem. Reprinted with permission from Advanced Electronic Materials. The data is from Naghibi, S., Kargar, F., Wright, D., Huang, C. Y. T., Mohammadzadeh, A., Barani, Z., Salgado, R. & Balandin, A. A. Noncuring Graphene Thermal Interface Materials for Advanced Electronics. *Advanced Electronic Materials* 1901303 (2020). doi:10.1002/aelm.201901303.

4.4 Benchmarking Against Commercial Noncuring TIMs

In order to benchmark the performance of the noncuring graphene thermal paste against the cutting edge TIM technology, we measured the “bulk” thermal conductivity of five top commercial TIMs widely used in industry. It should be noted that many commercial TIMs claim the thermal conductivity values exceeding $10 \text{ Wm}^{-1}\text{K}^{-1}$, although the vendor supplied descriptions do not specify how the thermal measurements have been performed. In Figure 4.8, we present the measured and claimed values of the “bulk” thermal conductivity of commercial TIMs. All measurements used the same experimental setup (s) under the same steady-state conditions at $35 \text{ }^\circ\text{C}$ and atmospheric pressure. The obtained data indicate that the true “bulk” thermal conductivity for all commercial noncuring TIMs is substantially lower than that specified in the vendor datasheets. The thermal conductivity of the noncuring graphene TIM with $\phi = 19.8 \text{ vol}\%$ surpasses that of the all commercial TIMs. The highest “bulk” thermal conductivity for the commercial noncuring TIM was obtained for TIM PK-Pro 3 (Prolimatech Inc.). It was determined to be $6.19 \text{ Wm}^{-1}\text{K}^{-1}$, which is close to the thermal conductivity of the noncuring graphene TIM. However, one should note that PK-Pro 3 incorporates $\sim 90 \text{ wt}\%$ of Al and ZnO as fillers⁷³ while graphene TIMs includes only $40 \text{ wt}\%$ of graphene (see Figure 4.8).

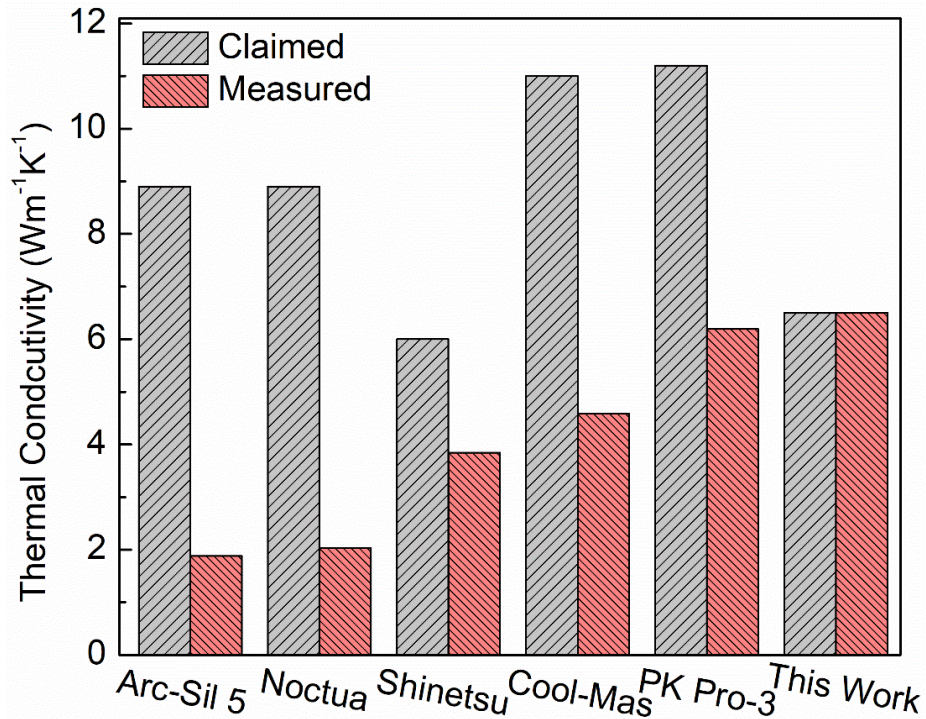


Figure 4.8: Benchmarking of noncuring graphene TIMs against commercial noncuring TIMs. The noncuring graphene TIM has $\phi = 19.8$ vol% (40 wt%) filler loading. The grey bars show the thermal conductivity values claimed by the vendors. The light coral bars present the data measured by the same instrument used for this study. There is a substantial discrepancy between the claimed and measured data for the commercial TIMs. The noncuring graphene thermal paste outperforms all commercial noncuring TIMs. A commercial noncuring TIM with the highest thermal conductivity (PK Pro-3) uses ~90 wt% of Al and ZnO filler loading, which is more than two times of the graphene filler concentration used in this study. Reprinted with permission from Advanced Electronic Materials. The data is from Naghibi, S., Kargar, F., Wright, D., Huang, C. Y. T., Mohammadzadeh, A., Barani, Z., Salgado, R. & Balandin, A. A. Noncuring Graphene Thermal Interface Materials for Advanced Electronics. *Advanced Electronic Materials* 1901303 (2020). doi:10.1002/aelm.201901303.

Table 4.1 summarizes recent research data for noncuring TIMs and nano-fluids with different fillers and host matrices. The difficulty in uniform dispersion of fillers through the matrix could be one of the reasons for the scarcity of literature in the field of noncuring thermal interface materials. The data presented in Figure 4.8 and Table 4.1 attest

for the great potential of noncuring graphene thermal paste for thermal management of advanced electronics.

Table 4.1: Thermal conductivity of noncuring thermal interface materials with different fillers.

Filler	Base Matrix	Filler Loading		Method	K ($Wm^{-1}K^{-1}$)	Refs.
		vol.%	wt %			
Graphene	Mineral Oil	27	50	TIM tester	7.1	This work
Al ₂ O ₃ / Graphene	Silicone grease	6/1	-	TPS	3.0	17
Graphene	Epoxy without resin	11	-	TIM tester	0.90	74
rGO	Silicone Oil	4.3	-	THWM	1	75
Graphene NF	Silicone Oil	4.3	-	THWM	0.25	75
Graphene	Silicone Oil	0.07	-	THWM	0.215	76
Graphene / CuO	Water	0.07	-	Kd2 thermometer	0.28	77
Graphene / Fe ₃ O ₄	Commercial TIM	-	6	Laser flash	~1.46	46
Functionalized Graphene	Water	-	5	THWM	1.15	78
GNP	Silicone Grease	0.75	-	THB	3.2	79
GNP	Water	-	0.10	THWM	0.75	80
CNT	Silicone Elastomer	-	4	TIM Tester	1.8	18
Silica	water	3	-	THWM	0.66	81
CuO microdisks	Silicone Base	0.09	-	Hot disk	0.28	20
CuO nanoblock	Silicone Base	0.09	-	Hot disk	0.25	20
CuO microspheres	Silicone Base	0.09	-	Hot disk	0.23	82
TiO ₂	Water	5	-	THWM	0.871	83
AlN	EG, PG	10	-	THWM	0.35	13
T- ZnO	Silicone Oil	18	-	TPS	0.88	19

NF = nano-flakes, GNP = graphene nano-platelets, EG = Ethylene Glycol, PG = Propylene Glycol
 THWM = transient hot wire method, TPS = Transient plane source THB = transient hot bridge

4.5 Conclusion

We reported on the synthesis and thermal conductivity measurements of noncuring thermal paste, i.e. grease, based on mineral oil with the mixture of graphene and few-layer graphene flakes as the fillers. It was found that graphene thermal paste exhibits a distinctive thermal percolation threshold with the thermal conductivity revealing a sublinear dependence on the filler loading. This behavior contrasts with the thermal conductivity of curing graphene thermal interface materials, based on epoxy, where super-linear dependence on the filler loading is observed. The performance of graphene thermal paste was benchmarked against top-of-the-line commercial thermal pastes. The obtained results show that noncuring graphene thermal interface materials outperforms the best commercial pastes in terms of thermal conductivity, at substantially lower filler concentration. The obtained results shed light on thermal percolation mechanism in noncuring polymeric matrices laden with quasi-two-dimensional fillers. Considering recent progress in graphene production *via* liquid phase exfoliation and oxide reduction, we argue that our results open a pathway for large-scale industrial application of graphene in thermal management of electronics.

References

1. Smoyer, J. L. & Norris, P. M. Brief Historical Perspective in Thermal Management and the Shift Toward Management at the Nanoscale. *Heat Transfer Engineering* **40**, 269–282 (2019).
2. Kargar, F., Barani, Z., Balinskiy, M., Magana, A. S., Lewis, J. S. & Balandin, A. A. Dual-Functional Graphene Composites for Electromagnetic Shielding and Thermal Management. *Advanced Electronic Materials* **10**, 37555–37565 (2018).
3. Kargar, F., Barani, Z., Salgado, R., Debnath, B., Lewis, J. S., Aytan, E., Lake, R. K. & Balandin, A. A. Thermal Percolation Threshold and Thermal Properties of Composites with High Loading of Graphene and Boron Nitride Fillers. *ACS Applied Materials & Interfaces* **10**, 37555–37565 (2018).
4. Cola, B. a., Xu, X. & Fisher, T. S. Increased Real Contact in Thermal Interfaces: A Carbon Nanotube/Foil Material. *Applied physics letters* **90**, 88–91 (2007).
5. Mu, L., Ji, T., Chen, L., Mehra, N., Shi, Y. & Zhu, J. Paving the Thermal Highway with Self-Organized Nanocrystals in Transparent Polymer Composites. *ACS Applied Materials and Interfaces* **8**, 29080–29087 (2016).
6. Lewis, J. S., Barani, Z., Magana, A. S., Kargar, F. & Balandin, A. A. Thermal and Electrical Conductivity Control in Hybrid Composites with Graphene and Boron Nitride Fillers. *Materials Research Express* **6**, 085325 (2019).
7. Teng, C.-C., Ma, C.-C. M., Lu, C.-H., Yang, S.-Y., Lee, S.-H., Hsiao, M.-C., Yen, M.-Y., Chiou, K.-C. & Lee, T.-M. Thermal Conductivity and Structure of Non-Covalent Functionalized Graphene/Epoxy Composites. *Carbon* **49**, 5107–5116 (2011).
8. Data Centers and Servers | Department of Energy. at <https://www.energy.gov/eere/buildings/data-centers-and-servers>
9. Gwinn, J. P. & Webb, R. L. Performance and Testing of Thermal Interface Materials. in *Microelectronics Journal* **34**, 215–222 (2003).
10. Bar-Cohen, A., Matin, K. & Narumanchi, S. Nanothermal Interface Materials: Technology Review and Recent Results. *Journal of Electronic Packaging* **137**, 040803 (2015).
11. Barani, Z., Mohammadzadeh, A., Geremew, A., Huang, C., Coleman, D., Mangolini, L., Kargar, F. & Balandin, A. A. Thermal Properties of the Binary-Filler Hybrid Composites with Graphene and Copper Nanoparticles. *Advanced Functional Materials* **30**, 1904008 (2020).

12. Xie, X., Li, D., Tsai, T.-H., Liu, J., Braun, P. V. & Cahill, D. G. Thermal Conductivity, Heat Capacity, and Elastic Constants of Water-Soluble Polymers and Polymer Blends. *Macromolecules* **49**, 972–978 (2016).
13. Yu, W., Xie, H., Li, Y. & Chen, L. Experimental Investigation on Thermal Conductivity and Viscosity of Aluminum Nitride Nanofluid. *Particuology* **9**, 187–191 (2011).
14. Zeng, J. L., Cao, Z., Yang, D. W., Sun, L. X. & Zhang, L. Thermal Conductivity Enhancement of Ag Nanowires on an Organic Phase Change Material. in *Journal of Thermal Analysis and Calorimetry* **101**, 385–389 (2010).
15. Murshed, S. M. S., Leong, K. C. & Yang, C. Enhanced Thermal Conductivity of TiO₂ - Water Based Nanofluids. *International Journal of Thermal Sciences* **44**, 367–373 (2005).
16. Wong, C. P. & Bollampally, R. S. Thermal Conductivity, Elastic Modulus, and Coefficient of Thermal Expansion of Polymer Composites Filled with Ceramic Particles for Electronic Packaging. *Journal of Applied Polymer Science* **74**, 3396–3403 (1999).
17. Yu, W., Xie, H., Yin, L., Zhao, J., Xia, L. & Chen, L. Exceptionally High Thermal Conductivity of Thermal Grease: Synergistic Effects of Graphene and Alumina. *International Journal of Thermal Sciences* **91**, 76–82 (2015).
18. Chen, H., Wei, H., Chen, M., Meng, F., Li, H. & Li, Q. Enhancing the Effectiveness of Silicone Thermal Grease by the Addition of Functionalized Carbon Nanotubes. *Applied Surface Science* **283**, 525–531 (2013).
19. Du, H., Qi, Y., Yu, W., Yin, J. & Xie, H. T-shape ZnO whisker: A More Effective Thermal Conductive Filler than Spherical Particles for the Thermal Grease. *International Journal of Heat and Mass Transfer* **112**, 1052–1056 (2017).
20. Yu, W., Zhao, J., Wang, M., Hu, Y., Chen, L. & Xie, H. Thermal Conductivity Enhancement in Thermal Grease Containing Different CuO Structures. *Nanoscale research letters* **10**, 113 (2015).
21. Cola, B. A., Xu, X. & Fisher, T. S. Increased Real Contact in Thermal Interfaces: A Carbon Nanotube/Foil Material. *Applied Physics Letters* **90**, 093513 (2007).
22. Initial hype passed, graphene shows up in real products. at <<https://www.canadianbusiness.com/innovation/graphene-after-the-hype/>>
23. Graphene thermal conductivity - introduction and latest news | Graphene-Info. at <<https://www.graphene-info.com/graphene-thermal>>

24. Novoselov, K. S., Geim, A. K., Morozov, S. V, Jiang, D., Zhang, Y., Dubonos, S. V., Grigorieva, I. V & Firsov, A. A. Electric Field Effect in Atomically Thin Carbon Films Supplementary. *Science* **5**, 1–12 (2004).
25. Geim, A. K. & Novoselov, K. S. The Rise of Graphene. *Nature Materials* **6**, 183–191 (2007).
26. Shao, Q., Liu, G., Teweldebrhan, D. & Balandin, A. A. Higherature Quenching of Electrical Resistance in Graphene Interconnects. *Applied Physics Letters* **92**, (2008).
27. Schwierz, F. Graphene Transistors. *Nature Nanotechnology* **5**, 487–496 (2010).
28. Yang, X., Liu, G., Balandin, A. A. & Mohanram, K. Triple-Mode Single-Transistor Graphene Amplifier and Its Applications. *ACS Nano* **4**, 5532–5538 (2010).
29. Yang, X., Liu, G., Rostami, M., Balandin, A. A. & Mohanram, K. Graphene Ambipolar Multiplier Phase Detector. *IEEE Electron Device Letters* **32**, 1328–1330 (2011).
30. Liu, G., Ahsan, S., Khitun, A. G., Lake, R. K. & Balandin, A. A. Graphene-Based Non-Boolean Logic Circuits. *Journal of Applied Physics* **114**, 154310 (2013).
31. Balandin, A. A. Thermal Properties of Graphene and Nanostructured Carbon Materials. *Nature Materials* **10**, 569–581 (2011).
32. Balandin, A. A., Ghosh, S., Bao, W., Calizo, I., Teweldebrhan, D., Miao, F. & Lau, C. N. Superior Thermal Conductivity of Single-Layer Graphene. *Nano Letters* **8**, 902–907 (2008).
33. Li, H., Ying, H., Chen, X., Nika, D. L., Cocemasov, A. I., Cai, W., Balandin, A. A. & Chen, S. Thermal Conductivity of Twisted Bilayer Graphene. *Nanoscale* **6**, 13402–13408 (2014).
34. Nika, D. L., Pokatilov, E. P., Askerov, A. S. & Balandin, A. A. Phonon Thermal Conduction in Graphene: Role of Umklapp and Edge Roughness Scattering. *Physical Review B - Condensed Matter and Materials Physics* **79**, 155413 (2009).
35. Nika, D. L., Ghosh, S., Pokatilov, E. P. & Balandin, A. A. Lattice Thermal Conductivity of Graphene Flakes: Comparison with Bulk Graphite. *Applied Physics Letters* **94**, 203103 (2009).
36. Nika, D. L., Askerov, A. S. & Balandin, A. A. Anomalous Size Dependence of the Thermal Conductivity of Graphene Ribbons. *Nano Letters* **12**, 3238–3244 (2012).
37. Hernandez, Y., Nicolosi, V., Lotya, M., Blighe, F. M., Sun, Z., De, S., McGovern, I. T., Holland, B., Byrne, M., Gun'Ko, Y. K., Boland, J. J., Niraj, P., Duesberg, G.,

- Krishnamurthy, S., Goodhue, R., Hutchison, J., Scardaci, V., Ferrari, A. C. & Coleman, J. N. High-yield Production of Graphene by Liquid-Phase Exfoliation of Graphite. *Nature Nanotechnology* **3**, 563–568 (2008).
38. Lotya, M., Hernandez, Y., King, P. J., Smith, R. J., Nicolosi, V., Karlsson, L. S., Blighe, F. M., De, S., Wang, Z., McGovern, I. T., Duesberg, G. S. & Coleman, J. N. Liquid Phase Production of Graphene by Exfoliation of Graphite in Surfactant/Water Solutions. *Journal of the American Chemical Society* **131**, 3611–3620 (2009).
 39. Stankovich, S., Dikin, D. A., Piner, R. D., Kohlhaas, K. A., Kleinhammes, A., Jia, Y., Wu, Y., Nguyen, S. T. & Ruoff, R. S. Synthesis of Graphene-based Nanosheets via Chemical Reduction of Exfoliated Graphite Oxide. *Carbon* **45**, 1558–1565 (2007).
 40. Stankovich, S., Dikin, D. A., Dommett, G. H. B., Kohlhaas, K. M., Zimney, E. J., Stach, E. A., Piner, R. D., Nguyen, S. B. T. & Ruoff, R. S. Graphene-based Composite Materials. *Nature* **442**, 282–286 (2006).
 41. Nethravathi, C. & Rajamathi, M. Chemically Modified Graphene Sheets Produced by the Solvothermal Reduction of Colloidal Dispersions of Graphite Oxide. *Carbon* **46**, 1994–1998 (2008).
 42. Shahil, K. M. F. & Balandin, A. A. Graphene–Multilayer Graphene Nanocomposites as Highly Efficient Thermal Interface Materials. *Nano Letters* **12**, 861–867 (2012).
 43. Shahil, K. M. F. & Balandin, A. A. Thermal Properties of Graphene and Multilayer Graphene: Applications in Thermal Interface Materials. *Solid State Communications* **152**, 1331–1340 (2012).
 44. Hansson, J., Zandén, C., Ye, L. & Liu, J. Review of Current Progress of Thermal Interface Materials for Electronics Thermal Management Applications. in *16th International Conference on Nanotechnology - IEEE NANO 2016* 371–374 (2016). doi:10.1109/NANO.2016.7751383
 45. Goyal, V. & Balandin, A. A. Thermal Properties of the Hybrid Graphene-Metal Nano-Micro-Composites: Applications in Thermal Interface Materials. *Applied Physics Letters* **100**, 073113 (2012).
 46. Renteria, J., Legedza, S., Salgado, R., Balandin, M. P., Ramirez, S., Saadah, M., Kargar, F. & Balandin, A. A. Magnetically-Functionalized Self-Aligning Graphene Fillers for High-Efficiency Thermal Management Applications. *Materials and Design* **88**, 214–221 (2015).

47. Kargar, F., Salgado, R., Legedza, S., Renteria, J. & Balandin, A. A. A Comparative Study of The Thermal Interface Materials with Graphene and Boron Nitride Fillers. in *Carbon Nanotubes, Graphene, and Associated Devices VII* **9168**, 91680S (SPIE, 2014).
48. Nair, R. R., Blake, P., Grigorenko, A. N., Novoselov, K. S., Booth, T. J., Stauber, T., Peres, N. M. R. & Geim, A. K. Fine Structure Constant Defines Visual Transparency of Graphene. *Science* **320**, 1308 (2008).
49. Ma, T., Zhao, Y., Ruan, K., Liu, X., Zhang, J., Guo, Y., Yang, X., Kong, J. & Gu, J. Highly Thermal Conductivities, Excellent Mechanical Robustness and Flexibility, and Outstanding Thermal Stabilities of Aramid Nanofiber Composite Papers with Nacre-Mimetic Layered Structures. *ACS Applied Materials & Interfaces* **12**, 1677–1686 (2020).
50. Hou, X., Chen, Y., Lv, L., Dai, W., Zhao, S., Wang, Z., Fu, L., Lin, C.-T., Jiang, N. & Yu, J. High-Thermal-Transport-Channel Construction within Flexible Composites via the Welding of Boron Nitride Nanosheets. *ACS Applied Nano Materials* **2**, 360–368 (2019).
51. Yu, A., Ramesh, P., Itkis, M. E., Bekyarova, E. & Haddon, R. C. Graphite Nanoplatelet-Epoxy Composite Thermal Interface Materials. *Journal of Physical Chemistry C* **111**, 7565–7569 (2007).
52. Gu, J., Xie, C., Li, H., Dang, J., Geng, W. & Zhang, Q. Thermal Percolation Behavior of Graphene Nanoplatelets/Polyphenylene Sulfide Thermal Conductivity Composites. *Polymer Composites* **35**, 1087–1092 (2014).
53. Yang, X., Liang, C., Ma, T., Guo, Y., Kong, J., Gu, J., Chen, M. & Zhu, J. A Review on Thermally Conductive Polymeric Composites: Classification, Measurement, Model and Equations, Mechanism and Fabrication Methods. *Advanced Composites and Hybrid Materials* **1**, 207–230 (2018).
54. Arao, Y., Mizuno, Y., Araki, K. & Kubouchi, M. Mass Production of High-Aspect-Ratio Few-Layer-Graphene by High-Speed Laminar Flow. *Carbon* **102**, 330–338 (2016).
55. Schneider, G. F., Xu, Q., Hage, S., Luik, S., Spoor, J. N. H., Malladi, S., Zandbergen, H. & Dekker, C. Tailoring the Hydrophobicity of Graphene for its use as Nanopores for DNA Translocation. *Nature Communications* **4**, (2013).
56. Xu, X., Pereira, L. F. C., Wang, Y., Wu, J., Zhang, K., Zhao, X., Bae, S., Tinh Bui, C., Xie, R., Thong, J. T. L., Hong, B. H., Loh, K. P., Donadio, D., Li, B. & Özyilmaz, B. Length-Dependent Thermal Conductivity in Suspended Single-Layer Graphene. *Nature Communications* **5**, 3689 (2014).

57. *Characteristics of Thermal Interface Materials.* (2001). at <<http://multimedia.3m.com/mws/media/122268O/characteristics-of-thermal-interface-materials.pdf>>
58. Bonnet, P., Sireude, D., Garnier, B. & Chauvet, O. Thermal Properties and Percolation in Carbon Nanotube-Polymer Composites. *Applied Physics Letters* **91**, 201910 (2007).
59. Zhang, L., Ruesch, M., Zhang, X., Bai, Z. & Liu, L. Tuning Thermal Conductivity of Crystalline Polymer Nanofibers by Interchain Hydrogen Bonding. *RSC Advances* **5**, 87981–87986 (2015).
60. Mu, L., Ji, T., Chen, L., Mehra, N., Shi, Y. & Zhu, J. Paving the Thermal Highway with Self-Organized Nanocrystals in Transparent Polymer Composites. **8**, 29080–29087 (2016).
61. Evans, W., Prasher, R., Fish, J., Meakin, P., Phelan, P. & Keblinski, P. Effect of Aggregation and Interfacial Thermal Resistance on Thermal Conductivity of Nanocomposites and Colloidal Nanofluids. *International Journal of Heat and Mass Transfer* **51**, 1431–1438 (2008).
62. Prasher, R. S., Shipley, J., Prstic, S., Koning, P. & Wang, J. lin. Thermal Resistance of Particle Laden Polymeric Thermal Interface Materials. in *American Society of Mechanical Engineers, Electronic and Photonic Packaging, EPP* **3**, 431–439 (2003).
63. Balandin, A. A. Thermal Properties of Graphene and Nanostructured Carbon Materials. *Nature Materials* **10**, 569–581 (2011).
64. Goyal, V. & Balandin, A. A. Thermal Properties of the Hybrid Graphene-Metal Nano-Micro-Composites: Applications in Thermal Interface Materials. *Applied Physics Letters* **100**, 073113 (2012).
65. Park, W., Guo, Y., Li, X., Hu, J., Liu, L., Ruan, X. & Chen, Y. P. High-Performance Thermal Interface Material Based on Few-Layer Graphene Composite. *The Journal of Physical Chemistry C* **119**, 26753–26759 (2015).
66. Zhong, Y., Zhou, M., Huang, F., Lin, T. & Wan, D. Effect of Graphene Aerogel on Thermal Behavior of Phase Change Materials for Thermal Management. *Solar Energy Materials and Solar Cells* **113**, 195–200 (2013).
67. Skuriat, R., Li, J. F., Agyakwa, P. A., Matthey, N., Evans, P. & Johnson, C. M. Degradation of Thermal Interface Materials for High-Temperature Power Electronics Applications. *Microelectronics Reliability* **53**, 1933–1942 (2013).

68. Hurley, S., Cann, P. M. & Spikes, H. A. Lubrication and Reflow Properties of Thermally Aged Greases. *Tribology Transactions* **43**, 221–228 (2000).
69. Gao, J., Mwasame, P. M. & Wagner, N. J. Thermal Rheology and Microstructure of Shear Thickening Suspensions of Silica Nanoparticles Dispersed in the Ionic Liquid [C 4 mim][BF 4]. *Journal of Rheology* **61**, 525–535 (2017).
70. Gowda, A., Esler, D., Paisner, S. N., Tonapi, S., Nagarkar, K. & Srihari, K. Reliability Testing of Silicone-Based Thermal Greases. in *Annual IEEE Semiconductor Thermal Measurement and Management Symposium* 64–71 (2005). doi:10.1109/stherm.2005.1412160
71. Li, J., Myllykoski, P. & Paulasto-Krockel, M. Study on Thermomechanical Reliability of Power Modules and Thermal Grease Pump-out Mechanism. in *2015 16th International Conference on Thermal, Mechanical and Multi-Physics Simulation and Experiments in Microelectronics and Microsystems, EuroSimE 2015* (2015). doi:10.1109/EuroSimE.2015.7103076
72. Chiu, C. P., Chandran, B., Mello, M. & Kelley, K. An Accelerated Reliability Test Method to Predict Thermal Grease Pump-Out in Flip-Chip Applications. *Proceedings - Electronic Components and Technology Conference* 91–97 (2001). doi:10.1109/ECTC.2001.927696
73. Prolimatech. at <<http://www.prolimatech.com/en/>>
74. Tian, X., Itkis, M. E., Bekyarova, E. B. & Haddon, R. C. Anisotropic Thermal and Electrical Properties of Thin Thermal Interface Layers of Graphite Nanoplatelet-Based Composites. *Scientific Reports* **3**, 1710 (2013).
75. Yu, W., Xie, H., Chen, L., Zhu, Z., Zhao, J. & Zhang, Z. Graphene Based Silicone Thermal Greases. *Physics Letters A* **378**, 207–211 (2014).
76. Ma, W., Yang, F., Shi, J., Wang, F., Zhang, Z. & Wang, S. Silicone Based Nanofluids Containing Functionalized Graphene Nanosheets. *Colloids and Surfaces A: Physicochemical and Engineering Aspects* **431**, 120–126 (2013).
77. Baby, T. T. & Sundara, R. Synthesis and Transport Properties of Metal Oxide Decorated Graphene Dispersed Nanofluids. *The Journal of Physical Chemistry C* **115**, 8527–8533 (2011).
78. Ghozatloo, A., Shariaty-Niasar, M. & Rashidi, A. M. Preparation of Nanofluids from Functionalized Graphene by New Alkaline Method and Study on the Thermal Conductivity and Stability. *International Communications in Heat and Mass Transfer* **42**, 89–94 (2013).

79. Phuong, M.T.; Trinh, P.V.; Tuyen, N.V.; Dinh, N.N.; Minh, P.N.; Dung, N.D.; Thang, B. H. Effect of Graphene Nanoplatelet Concentration on the Thermal Conductivity of Silicone Thermal Grease. *Physics, Journal of Nano- and Electronic* **11**, 5039 (2019).
80. Mehrali, M., Sadeghinezhad, E., Latibari, S. T., Kazi, S. N., Mehrali, M., Zubir, M. N. B. M. & Metselaar, H. S. C. Investigation of Thermal Conductivity and Rheological Properties of Nanofluids Containing Graphene Nanoplatelets. *Nanoscale Research Letters* **9**, 15 (2014).
81. Ranjbarzadeh, R., Moradikazerouni, A., Bakhtiari, R., Asadi, A. & Afrand, M. An Experimental Study on Stability and Thermal Conductivity of Water/Silica Nanofluid: Eco-Friendly Production of Nanoparticles. *Journal of Cleaner Production* **206**, 1089–1100 (2019).
82. Yu, W., Zhao, J., Wang, M., Hu, Y., Chen, L. & Xie, H. Thermal Conductivity Enhancement in Thermal Grease Containing Different CuO Structures. *Nanoscale Research Letters* **10**, 113 (2015).
83. Murshed, S. M. S., Leong, K. C. & Yang, C. Enhanced Thermal Conductivity of TiO₂—Water Based Nanofluids. *International Journal of Thermal Sciences* **44**, 367–373 (2005).